Published OnlineFirst July 30, 2012; DOI:10.1158/1078-0432.CCR-12-0701

important role in modulating the sensitivity to chemotherapy such as cisplatin and 5-FU (24). In the present study, let-7 expression modulated the chemosensitivity to genotoxic chemotherapy in esophageal cancer through the IL-6/STAT3 pathway.

IL-6 is an inflammatory cytokine known to be released from macrophages and T lymphocytes as well as from cancer cells (25). Previous studies indicated that IL-6 is associated with resistance to chemotherapy in a variety of malignancies. In ovarian cancer, Wang and colleagues (26) reported that autocrine production of IL-6 confers resistance to cisplatin and paclitaxel. Iliopoulos and colleagues (18) reported that IL-6 plays a pivotal role in chemoresistance by inducing the conversion of non–cancer stem cells to cancer stem cells in breast cancer cells. With regard to esophageal cancer, one recent study showed that intracellular IL-6 expression after cisplatin exposure is associated with reduced sensitivity to cisplatin treatment and that knockdown of IL-6 expression restored sensitivity to cisplatin treatment. In the present study, we showed that esophageal cancer cells release IL-6 after exposure to cisplatin and that IL-6 activated prosurvival JAK/STAT3 pathway in an autocrine manner, leading to cisplatin resistance. On the other hand, another recent report by Gilbert and Hemann (27) showed that IL-6 secreted from endothelial cells after treatment with doxorubicin created chemoresistant niche and is involved in increased resistance to DNA damaging agents in paracrine manner. Indeed, we showed in this study that let-7 repressed IL-6 activation in esophageal cancer cells in an autocrine manner during chemotherapy, but we think that let-7 can inhibit IL-6 production from the surrounding normal cells such as fibroblasts, endothelial cells, and macrophages. Further studies are needed to clarify whether let-7 represses paracrine IL-6 signal in the surrounding normal tissues in addition to its effect on autocrine IL-6 production from cancer cells.

In this study, transfection of let-7c resulted in a significant reduction in phosphorylated STAT3 in the cells, but it did not induce any significant change in the expression of Akt and Erk. Indeed, Akt and Erk are considered to be downstream of IL-6, similar to STAT3, and to be involved in antiapoptotic pathway (26), although their expression can be regulated by upstream signals other than IL-6. For example, Akt expression is reported to be regulated by phosphoinositide 3-kinase (PI3K), mTOR, and phosphate and tensin homolog (PTEN) deleted from chromosome 10 (28–31). Erk expression is also reported to be regulated by several receptors protein tyrosine kinases and the mitogen-activated protein kinase (MAPK) pathway (32–35). One possible explanation for the lack of significant effect of let-7c transfection on Akt and Erk could be that Akt and Erk pathways are regulated mainly by signals other than IL-6 whereas STAT3 is regulated by IL-6 expression in esophageal cancer cells.

There is increasing evidence that let-7 inhibits IL-6 signaling pathway directly by targeting IL-6. Iliopoulos and colleagues (18) showed that NF-κB, Lin28, let-7, and IL-6 form an inflammatory positive feedback loop. NF-κB induces Lin28 expression, leading to inhibition of let-7 and expression of the encoding IL-6. IL-6 can itself activate NF-κB, resulting in a positive feedback loop. Another recent report showed that downregulation of let-7 promotes the expression of IL-6 and IL-10 during *Salmonella* infection. Thus, the association between let-7 and IL-6 under an inflammatory environment has been described, but this is the first time to show that the association between let-7 and IL-6 plays an important role in the sensitivity to chemotherapy for cancer. This result suggests that treatment targeting this pathway is likely to enhance the response to anticancer chemotherapy.

The present study has certain limitations. First, the clinical results were based on retrospective analysis by using biopsy samples obtained from patients who underwent preoperative chemotherapy followed by surgery at only one institution. Second, the current results that let-7 modulates the chemosensitivity in esophageal cancer through the regulation of IL-6/STAT3 pathway may be adapted into cisplatin-based chemotherapy but not other chemotherapeutic regimens that do not include cisplatin, because cisplatin-resistant cell line used in this study did not show resistance to 5-FU nor Adriamycin (data not shown). However, cisplatin-based chemotherapy is the most widely used chemotherapeutic regimen for esophageal cancer, although other chemotherapeutic regimens are used occasionally, such as taxane-based chemotherapy for esophageal cancer which has low expression of let-7. Third, before one can apply the findings that let-7 expression can be used clinically to predict the response of esophageal cancer to chemotherapy, we need to validate this result in a prospective multicenter clinical trial.

In summary, we showed that evaluation of let-7 b and let-7c expression before treatment is potentially useful to predict the response to chemotherapy in patients with esophageal cancer. Moreover, the results also showed that the effect of let-7 expression on chemosensitivity is mediated though downregulation of IL-6/STAT3 pathway. Further studies are needed to explore the therapeutic potential of the let-7/IL-6/STAT3 pathway in genotoxic anticancer therapy.

Disclosure of Potential Conflicts of Interest

No potential conflicts of interest were disclosed.

Authors' Contributions

Conception and design: K. Sugimura, H. Miyata, R. Hamano, M. Mori, Y. Doki

Development of methodology: K. Sugimura, H. Miyata, R. Hamano, M. Mori, Y. Doki

Acquisition of data (provided animals, acquired and managed patients, provided facilities, etc.): K. Sugimura, H. Miyata, K. Tanaka, R. Hamano, T. Takahashi, Y. Kurokawa, M. Yamasaki, K. Nakajima, S. Takiguchi, M. Mori, Y, Doki

Analysis and interpretation of data (e.g., statistical analysis, biostatistics, computational analysis): K. Sugimura, H. Miyata, K. Tanaka, M. Yamasaki, M. Mori

Writing, review, and/or revision of the manuscript: K. Sugimura, H. Miyata, K. Tanaka, R. Hamano, T. Takahashi, Y. Kurokawa, M. Yamasaki, K. Nakajima, S. Takiguchi, M. Mori, Y, Doki

Administrative, technical, or material support (i.e., reporting or organizing data, constructing databases): K. Sugimura, H. Miyata, T. Takahashi, M. Yamasaki

Published OnlineFirst July 30, 2012; DOI:10.1158/1078-0432.CCR-12-0701

Study supervision: K. Sugimura, H. Miyata, K. Tanaka, R. Hamano, T. Takahashi, Y. Kurokawa, M. Yamasaki, K. Nakajima, S. Takiguchi, M. Mori, Y. Doki

The costs of publication of this article were defrayed in part by the payment of page charges. This article must therefore be hereby marked *advertisement* in accordance with 18 U.S.C. Section 1734 solely to indicate this fact.

Received February 28, 2012; revised June 12, 2012; accepted July 10, 2012; published OnlineFirst July 30, 2012.

References

1. Lerut T, Nafteux P, Moons J, Coosemans W, Decker G, De Leyn P, et al. Three-field lymphadenectomy for carcinoma of the esophagus and gastroesophageal junction in 174 R0 resections: impact on staging, disease-free survival, and outcome: a plea for adaptation of TNM classification in upper-half esophageal carcinoma. Ann Surg 2004;240:962–72; discussion 972–4.
2. Walsh TN, Noonan N, Hollywood D, Kelly A, Keeling N, Hennessy TP. A comparison of multimodal therapy and surgery for esophageal adenocarcinoma. N Engl J Med 1996;335:462–7.
3. Gebski V, Burmeister B, Smithers BM, Foo K, Zalcberg J, Simes J. Survival benefits from neoadjuvant chemoradiotherapy or chemotherapy in oesophageal carcinoma: a meta-analysis. Lancet Oncol 2007;8:226–34.
4. Iizuka T, Kakegawa T, Ide H, Ando N, Watanabe H, Tanaka O, et al. Phase II evaluation of cisplatin and 5-fluorouracil in advanced squamous cell carcinoma of the esophagus: a Japanese Esophageal Oncology Group Trial. Jpn J Clin Oncol 1992;22:172–6.
5. Polee MB, Kok TC, Siersema PD, Tilanus HW, Splinter TA, Stoter G, et al. Phase II study of the combination cisplatin, etoposide, 5-fluorouracil and folinic acid in patients with advanced squamous cell carcinoma of the esophagus. Anticancer Drugs 2001;12:513–7.
6. Takahashi H, Arimura Y, Yamashita K, Okahara S, Tanuma T, Kodaira J, et al. Phase I/II study of docetaxel/cisplatin/fluorouracil combination chemotherapy against metastatic esophageal squamous cell carcinoma. J Thorac Oncol 2010;5:122–8.
7. Yamasaki M, Miyata H, Tanaka K, Shiraishi O, Motoori M, Peng YF, et al. Multicenter phase I/II study of docetaxel, cisplatin and fluorouracil combination chemotherapy in patients with advanced or recurrent *squamous cell carcinoma of the esophagus. Oncology* 2011;80:307–13.
8. Miyata H, Yoshioka A, Yamasaki M, Nushijima Y, Takiguchi S, Fujiwara Y, et al. Tumor budding in tumor invasive front predicts prognosis and survival of patients with esophageal squamous cell carcinomas receiving neoadjuvant chemotherapy. Cancer 2009;115:3324–34.
9. Bartel DP. MicroRNAs: genomics, biogenesis, mechanism, and function. Cell 2004;116:281–97.
10. Croce CM, Calin GA. miRNAs, cancer, and stem cell division. Cell 2005;122:6–7.
11. Mathe EA, Nguyen GH, Bowman ED, Zhao Y, Budhu A, Schetter AJ, et al. MicroRNA expression in squamous cell carcinoma and adenocarcinoma of the esophagus: associations with survival. Clin Cancer Res 2009;15:6192–200.
12. Feber A, Xi L, Luketich JD, Pennathur A, Landreneau RJ, Wu M, et al. MicroRNA expression profiles of esophageal cancer. J Thorac Cardiovasc Surg 2008;135:255–60.
13. Giovannetti E, Funel N, Peters GJ, Del Chiaro M, Erozenci LA, Vasile E, et al. MicroRNA-21 in pancreatic cancer: correlation with clinical outcome and pharmacologic aspects underlying its role in the modulation of gemcitabine activity. Cancer Res 2010;70:4528–38.
14. Hamano R, Miyata H, Yamasaki M, Kurokawa Y, Hara J, Moon JH, et al. Overexpression of miR-200c induces chemoresistance in esophageal cancers mediated through activation of the Akt signaling pathway. Clin Cancer Res 2011;17:3029–38
15. Miller AB, Hoogstraten B, Staquet M, Winkler A. Reporting results of cancer treatment. Cancer 1981;47:207–14.
16. Japanese Society for Esophageal Diseases. Japanese classification of esophageal cancer. 10th ed. Tokyo, Japan: Kanehara & Co Ltd.; 2008.
17. Livak KJ, Schmittgen TD. Analysis of relative gene expression data using real-time quantitative PCR and the 2(-delta delta C(T)) method. Methods 2001;25:402–8.
18. Iliopoulos D, Hirsch HA, Struhl K. An epigenetic switch involving NF-kappaB, Lin28, Let-7 MicroRNA, and IL6 links inflammation to cell transformation. Cell 2009;139:693–706.
19. Poth KJ, Guminski AD, Thomas GP, Leo PJ, Jabbar IA, Saunders NA. Cisplatin treatment induces a transient increase in tumorigenic potential associated with high interleukin-6 expression in head and neck squamous cell carcinoma. Mol Cancer Ther 2010;9:2430–9.
20. Yang N, Kaur S, Volinia S, Greshock J, Lassus H, Hasegawa K, et al. MicroRNA microarray identifies Let-7i as a novel biomarker and therapeutic target in human epithelial ovarian cancer. Cancer Res 2008;68:10307–14.
21. Nakajima G, Hayashi K, Xi Y, Kudo K, Uchida K, Takasaki K, et al. Non-coding MicroRNAs hsa-let-7g and hsa-miR-181b are associated with chemoresponse to S-1 in colon cancer. Cancer Genomics Proteomics 2006;3:317–24.
22. Li Y, VandenBoom TG II, Kong D, Wang Z, Ali S, Philip PA, et al. Up-regulation of miR-200 and let-7 by natural agents leads to the reversal of epithelial-to-mesenchymal transition in gemcitabine-resistant pancreatic cancer cells. Cancer Res 2009;69:6704–12.
23. Shimizu S, Takehara T, Hikita H, Kodama T, Miyagi T, Hosui A, et al. The let-7 family of microRNAs inhibits Bcl-xL expression and potentiates sorafenib-induced apoptosis in human hepatocellular carcinoma. J Hepatol 2010;52:698–704.
24. Yu CC, Chen YW, Chiou GY, Tsai LL, Huang PI, Chang CY, et al. MicroRNA let-7a represses chemoresistance and tumourigenicity in head and neck cancer via stem-like properties ablation. Oral Oncol 2011;47:202–10.
25. Bromberg J, Wang TC. Inflammation and cancer: IL-6 and STAT3 complete the link. Cancer Cell 2009;15:79–80.
26. Wang Y, Niu XL, Qu Y, Wu J, Zhu YQ, Sun WJ, et al. Autocrine production of interleukin-6 confers cisplatin and paclitaxel resistance in ovarian cancer cells. Cancer Lett 2010;295:110–23.
27. Gilbert LA, Hemann MT. DNA damage-mediated induction of a chemoresistant niche. Cell 2010;143:355–66.
28. Franke TF, Kaplan DR, Cantley LC. PI3K: downstream AKTion blocks apoptosis. Cell 1997;88:435–7.
29. Hay N, Sonenberg N. Upstream and downstream of mTOR. Genes Dev 2004;18:1926–45.
30. Hay N. The Akt-mTOR tango and its relevance to cancer. Cancer Cell 2005;8:179–83.
31. Dubrovska A, Kim S, Salamone RJ, Walker JR, Maira SM, Garcia-Echeverria C, et al. The role of PTEN/Akt/PI3K signaling in the maintenance and viability of prostate cancer stem-like cell populations. Proc Natl Acad Sci U S A 2009;106:268–73.
32. Plowman GD, Sudarsanam S, Bingham J, Whyte D, Hunter T. The protein kinases of *Caenorhabditis elegans*: a model for signal transduction in multicellular organisms. Proc Natl Acad Sci U S A 1999;96:13603–10.
33. Schulze WX, Deng L, Mann M. Phosphotyrosine interactome of the ErbB-receptor kinase family. Mol Syst Biol 2005;1:20050008.
34. Friedman AA, Tucker G, Singh R, Yan D, Vinayagam A, Hu Y, et al. Proteomic and functional genomic landscape of receptor tyrosine kinase and ras to extracellular signal-regulated kinase signaling. Sci Signal 2011;4:10.
35. Gough NR. Focus issue: recruiting players for a game of ERK. Sci Signal 2011;4:9.

Ann Surg Oncol (2012) 19:S355–S364
DOI 10.1245/s10434-011-1797-x

Annals of
SURGICAL ONCOLOGY
OFFICIAL JOURNAL OF THE SOCIETY OF SURGICAL ONCOLOGY

ORIGINAL ARTICLE – TRANSLATIONAL RESEARCH AND BIOMARKERS

Role of the Hypoxia-Related Gene, JMJD1A, in Hepatocellular Carcinoma: Clinical Impact on Recurrence after Hepatic Resection

Daisaku Yamada, MD, Shogo Kobayashi, MD, PhD, Hirofumi Yamamoto, MD, PhD, Yoshito Tomimaru, MD, Takehiro Noda, MD, PhD, Mamoru Uemura, MD, PhD, Hiroshi Wada, MD, PhD, Shigeru Marubashi, MD, PhD, Hidetoshi Eguchi, MD, PhD, Masahiro Tanemura, MD, PhD, Yuichiro Doki, MD, PhD, Masaki Mori, MD, PhD, and Hiroaki Nagano, MD, PhD

Department of Surgery, Gastroenterological Surgery, Graduate School of Medicine, Osaka University, Suita, Osaka, Japan

ABSTRACT

Background and Aims. Intratumoral hypoxia affects every major aspect of cancer biology, but the relationship between hypoxia-induced genes and hepatocellular carcinoma has not been fully investigated. From a previously ranked microarray of hypoxia-inducible genes related to hepatocellular carcinoma, we focused on a histone H3 lysine 9 demethylase, known as Jumonji domain containing 1A. One function of this demethylase is to amplify hypoxia-inducible gene expression. We hypothesized that the demethylase would be a significant marker of hepatocellular carcinoma.

Methods. We examined Jumonji domain containing 1A expression in 110 hepatocellular carcinoma samples with quantitative real-time polymerase chain reaction and immunohistochemistry. We performed a small interfering RNA suppression analysis to determine the biological roles of the demethylase in proliferation, invasion, and the expression of epithelial–mesenchymal transition-related genes.

Results. The level of Jumonji domain containing 1A in cancer tissues was higher than in normal tissues ($P < 0.0001$). Protein expression was significantly related to gene expression ($P < 0.0001$). Samples with high Jumonji domain containing 1A expression ($n = 47$) had higher recurrence rates ($P = 0.0006$) than those with low expression. Multivariate Cox regression analysis revealed that Jumonji domain containing 1A expression was an independent predictor of recurrence ($P = 0.0016$), but was not significantly associated with any clinicopathological characteristics. Moreover, suppression of Jumonji domain containing 1A expression in hepatocellular carcinoma cell lines under hypoxic conditions reduced cell growth inhibition, reduced invasion ability, and arrested epithelial–mesenchymal transitions.

Conclusion. Jumonji domain containing 1A is a useful prognostic marker and may ameliorate malignant transformation in hepatocellular carcinoma.

Hepatocellular carcinoma (HCC) is the fifth most common cancer in the world. HCC causes 500,000 deaths globally each year, and its incidence is increasing worldwide, due to the dissemination of hepatitis B and C virus infections.[1] Advances in surgical techniques and perioperative care have greatly improved the outcome of hepatic resection for HCC.[2–4] Nonetheless, long-term survival after hepatectomy remains unsatisfactory, due to the high incidence of recurrence or metastasis. For these recurrent HCCs, inducing hypoxia by intercepting the hepatic arterial blood flow, i.e., transarterial chemoembolization (TACE), has achieved a pronounced therapeutic effect.[1,5] Although overall survival was prolonged after HCC treatment, success was transient in most patients. In some cases, high incidence of intrahepatic and/or distant metastases was observed after hepatic artery occlusion;[6–9] this suggested that hypoxia-inducible genes may play a role in increasing malignant potency in HCC.

Electronic supplementary material The online version of this article (doi:10.1245/s10434-011-1797-x) contains supplementary material, which is available to authorized users.

First Received: 8 March 2011;
Published Online: 24 May 2011

H. Nagano, MD, PhD
e-mail: hnagano@gesurg.med.osaka-u.ac.jp

Hypoxia is a characteristic feature of many solid tumors; it affects every major aspect of cancer biology, including cell invasion, recurrence, and metastasis.[10] In several cancers, poor prognosis is closely related to intratumoral hypoxia and/or expression of hypoxia-related endogenous proteins, including vascular endothelial growth factor, hypoxia-inducible factor-1, and glucose transporter 1.[11–16] It has been noted that, although hypoxia kills most tumor cells, it provides strong selective pressure for survival of the most aggressive and metastatic cells.[17] These cells proficiently escape the noxious hypoxic microenvironment by activating an invasive epithelial–mesenchymal transition (EMT), inducing angiogenesis, and promoting other metastatic programs that ultimately lead to tumor recurrence or metastasis.[18–23] In addition, hypoxia-inducible gene expression profiles have been associated with poor prognosis in human cancers.[23] Taken together, these data suggested that hypoxic conditions significantly affect HCC; however, it is unclear which hypoxia-inducible genes are most significantly related to HCC.[24]

We previously studied microarray data of liver metastases from colorectal cancer to identify hypoxia-inducible genes.[25] Of the 3,000 genes ranked in the microarray data, the top 30 were identified as hypoxia-inducible genes. Among the 30 genes, we focused on a histone H3, lysine 9 demethylase known as Jumonji domain containing 1A (JMJD1A). We showed that JMJD1A expression was a novel, independent, prognostic marker for colorectal cancer.[25] The functional relevance of JMJD1A has not been fully clarified, but it appears to cause transcriptional activation of various downstream target genes and amplifies hypoxia-inducible gene expression.[26–29] We confirmed that JMJD1A was induced in three HCC cell lines under hypoxic conditions. We hypothesized that JMJD1A was a significant gene activator and switch for an epigenetic pathway in hypoxic conditions; furthermore, JMJD1A expression may serve as a prognostic marker for HCC.

In this study, we aim to confirm the expression and localization of JMJD1A and assess its potential as a prognostic indicator in HCC by comparing its expression in HCC and liver background tissues. Moreover, we performed JMJD1A suppression analysis to determine whether JMJD1A might play a role in increasing the malignant potency of HCC cells under hypoxic conditions.

MATERIALS AND METHODS

Cell Lines and Culture

Human HCC cell lines (HuH7, PLC/PRF/5[PLC], and HepG2) were obtained from the Japan Cancer Research Resources Bank (Osaka, Japan). Cells were grown in Dulbecco's modified Eagle's medium supplemented with 10% fetal bovine serum, and 100 units/ml penicillin at 37°C in a humidified incubator with 5% CO_2. For hypoxic conditions, cells were grown for up to 72 h at 37°C in a continuously monitored atmosphere of 1% O2, 5% CO_2, and 94% N_2 in a multigas incubator (model 9200; Wakenyaku Co., Kyoto, Japan). Control/reference cells were cultured in normoxic conditions (21% O_2).

Clinical Samples

A total of 110 quality-verified HCC samples and paired noncancerous samples were obtained from patients who underwent liver resection from 2000 to 2005 at Osaka University Hospital. All patients were clearly diagnosed with HCC, based on clinicopathological findings. Mean age was 63.4 ± 0.9 years; male-to-female ratio was 89:21; tumor size was 5.1 ± 0.3 cm; and mean follow-up time was 32.6 ± 3.3 months. Patient clinicopathological features are presented in Table 2. During surgery, HCC and corresponding noncancerous tissue samples were immediately suspended in an RNA stabilization reagent (RNA Later; Ambion, Inc., Austin, TX) and stored at –80°C until RNA extraction. Other resected HCC specimens were preserved in paraffin blocks. The use of resected samples was approved by the Human Ethics Review Committee of the Graduate School of Medicine, Osaka University, and informed consent was obtained from each patient included in the study.

Immunohistochemistry

Immunohistochemical studies of JMJD1A were performed on 87 surgical specimens of HCC, as described previously.[30] Briefly, formalin-fixed, paraffin-embedded tissues were deparaffinized, microwaved for antigen retrieval, incubated with specific, rabbit polyclonal, anti-JMJD1A antibodies (1:100 dilution; Proteintech Group, Inc., Chicago, IL) for 1 h at room temperature, and detected with avidin–biotin complex reagents (Vector Laboratory Inc., Burlingame, CA) and diaminobenzidine. All sections were counterstained with hematoxylin. For negative controls, the primary antibody was substituted with nonimmunized immunoglobulin G (Vector Laboratories)

Western Blot Analysis

Western blot analysis was performed as described previously.[31] Briefly, total protein was extracted from HCC cell lines in radio immunoprecipitation assay (RIPA) buffer (Thermo Fisher Scientific, Inc., Rockford, IL). Aliquots of total protein (12 μg) were electrophoresed on sodium dodecyl sulfate polyacrylamide gel electrophoresis (SDS-PAGE), 10% Tris-HCl gels (Bio-Rad Laboratories Inc.,

Hercules, CA). The separated proteins were transferred to polyvinylidene difluoride membranes (Millipore Co., Billerica, MA) and incubated with primary antibodies for 1 h. Proteins were detected with the anti-JMJD1A antibody (diluted 1:800) and anti β-actin antibody (diluted 1:1,000; Sigma, Co., Tokyo, Japan).

qRT-PCR

Total RNA was isolated from cultured cells or tumor tissues with Trizol reagent (Invitrogen, Carlsbad, CA, USA) as previously described.[32] Complementary DNA was synthesized from 8.0 μg total RNA with the SuperScript first-strand synthesis system (Invitrogen), according to the manufacturer's protocol.

Real-time quantitative polymerase chain reactions (qRT-PCR) were conducted with the LightCycler-FastStart DNA Master SYBR Green I kit (Roche Applied Science) with the gene-specific oligonucleotide primers presented in Table 1.[25,30,32–34] Amplifications were performed in triplicate with the LightCycler system (Roche Applied Science, Indianapolis, IN) and the following protocol: initial denaturation at 95°C for10 min, followed by 45 cycles of 95°C for 10 s, 55°C for 10 s, and 60°C for 10 s. Melting curve analysis was performed to distinguish specific products from nonspecific products and primer dimers. Relative expression was calculated as the ratio of specific messenger RNA (mRNA) to endogenous β-actin mRNA in each sample.

Transfection of Small Interfering RNA (siRNA)

For siRNA suppression, we used a Stealth RNAi kit (Invitrogen, Carlsbad, CA) with double-stranded RNA duplexes that targeted human JMJD1A, (5-AGAAGA AUUCAAGAGAUUCCGGAGG-3/5-CCUCCGGAAUCU CUUGAAUUCUUCU-3), and negative control siRNA (NC), as previously described.[25] HCC cell lines were transfected with the siRNAs in lipofectamine RNAiMAX (Invitrogen), according to the manufacturer's protocols.

Proliferation and Invasion Assays

The proliferation assay was performed with a Cell Counting Kit-8 (Dojindo Molecular Technologies, Rockville, MD), as described previously.[35] Briefly, the viable cell number was determined by the absorbance value. We calculated the ratios of day 0 absorbance to day 1, 2 or 3 absorbance values. The invasion assay was performed with Transwell cell culture chambers (BD Biosciences, Bedford, MA), as described previously.[36] Briefly, 5×10^5 cells were seeded in triplicate on a Matrigel-coated membrane. After 48 h, cells that had invaded the undersurface of the membrane were fixed with 100% methanol and stained with 1% toluidine blue. Four microscopic fields were randomly selected for cell counting.

Statistical Analysis

Statistical analysis was performed with Student's *t*-test or Fisher's exact test for categorical data and the Mann–Whitney *U* test for nonparametric data. Correlation significance was assessed with Pearson's correlation coefficient test. Receiver operating characteristic (ROC) curves were established by plotting positive versus (1—negative) immunohistochemical samples. The Youden index (sensitivity + specificity − 1) was used to determine the optimal cutoff point for JMJD1A mRNA levels to predict disease-free survival.[37] The Kaplan–Meier analysis and the log-rank test were used to construct the disease-free survival curve and to evaluate differences. The prognostic value of each clinicopathologic characteristic was first determined by univariate Cox regression analysis. Parameters significantly related to survival on univariate analysis were included in multivariate analysis to identify significant clinicopathologic factors. *P*-values < 0.05 were considered statistically significant. All statistical analysis was carried out with JMP 8.0 software (SAS Institute, Tokyo, Japan).

RESULTS

Relationship between JMJD1A mRNA and Protein Expression

JMJD1A mRNA expression was significantly higher in HCC tissues ($1.03 \pm 2.67 \times 10^7$, mean ± SD; 2.82, median; $n = 110$) than in corresponding noncancerous tissues (0.133 ± 0.027; 0.119; $n = 21$) (Fig. 1a, $P < 0.0001$). JMJD1A protein expression was observed in 26 of 87 HCC

TABLE 1 Primers used for RT-PCR assay

Gene	Sense primer	Antisense primer
JMJD1A	5′-GCAAAGGACACGGAGAAGAT-3′	5′-CCCAGCCTTGAACTCCATAC-3′
E-cadherin	5′-TGCCCAGAAAATGAAAAAGG-3′	5′-GTGTATGTGGCAATGCGTTC-3′
N-cadherin	5′-TGAAACGCCGGGATAAAGAACG-3′	5′-TGCTGCAGCTGGCTCAAGTCAT-3′
Twist	5′-GGGAGTCCGCAGTCTTACGA-3′	5′-AGACCGAGAAGGCGTAGCTG-3′
β-Actin	5′-TTGTTACAGGAAGTCCCTTGCC-3′	5′-ATGCTATCACCTCCCCTGTGTG-3′

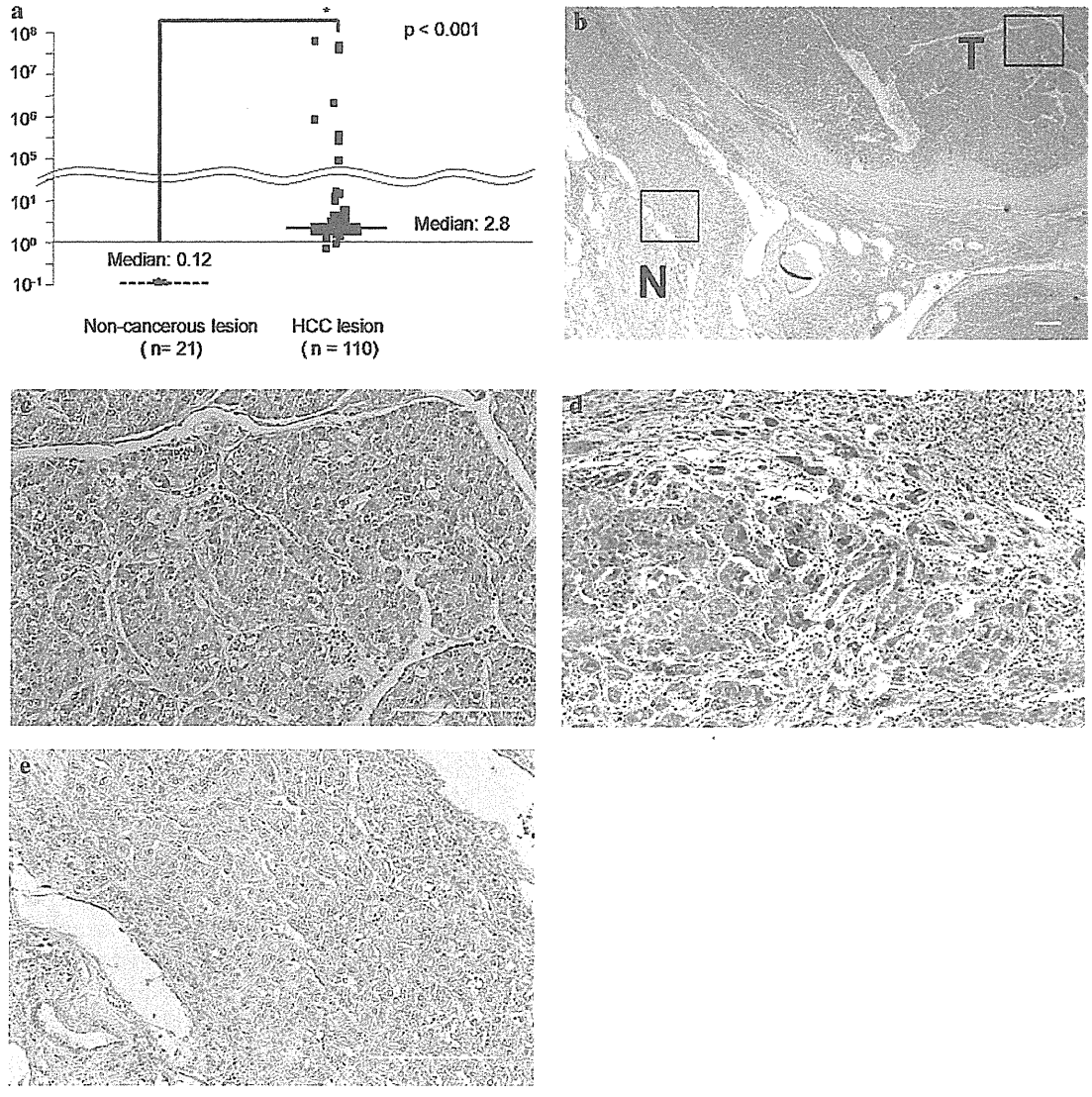

FIG. 1 JMJD1A mRNA and protein expression in resected HCC specimens. **a** JMJD1A mRNA expression determined by qRT-PCR. mRNA levels were normalized to endogenous β-actin mRNA (JMJD1A mRNA/β-actin mRNA) for expression in HCC tumors ($n = 110$) and noncancerous tissues ($n = 21$). Horizontal lines indicate median values for each group. **b–e** Representative immunohistochemical stains for JMJD1A: **b** HCC tissues (T) showed strong staining compared with corresponding noncancerous (N) tissues. **c, d** High-power fields showed that JMJD1A staining was localized in **c** the cytoplasm, and **d** both the nucleus and cytoplasm of HCC tissues. **e** JMJD1A was not detected in the corresponding noncancerous tissues. Scale bars 200 μm

tissues (Fig. 1b–d), but was not detected in corresponding noncancerous tissues (Fig. 1e). Of the 26 positively stained specimens, 22 showed staining only in the cytoplasm (Fig. 1c), and 4 showed staining in the nucleus and cytoplasm (Fig. 1d). In tissues positive for JMJD1A protein, the mRNA expression was higher than that observed in tissues negative for JMJD1A protein ($1.10 \pm 5.61 \times 10^7$ versus 2.97 ± 8.20, respectively; mean $\pm$ SD, $P < 0.0001$).

Based on the correlation between JMJD1A mRNA and protein expression, we grouped the specimens by high and low expression levels. To identify lesions with the highest positivity in both mRNA and protein, we used ROC curve analysis of protein reactivity to determine an appropriate cutoff value in the mRNA expression levels of corresponding samples (Supplementary Fig. 1). The area under the ROC curve was 0.893; the JMJD1A mRNA cutoff value of 2.15-fold gave sensitivity and specificity for positive JMJD1A protein reactivity of 84.6% and 80.3%, respectively. With this cutoff value, we divided HCC samples into JMJD1A-high ($n = 47$) and JMJD1A-low ($n = 63$) expression groups.

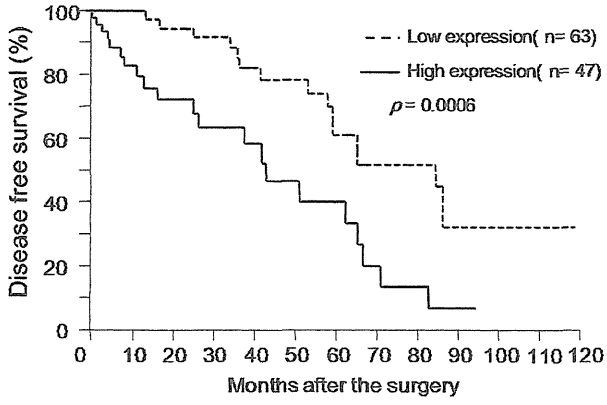

FIG. 2 Disease-free survival analysis according to protein and mRNA expression. Disease-free survival in patients with HCC after curative resection. Low and high JMJD1A expression was based on the cutoff value (2.15-fold) for mRNA expression

Patient Background and Survival in JMJD1A-High and JMJD1A-Low Groups

No significant differences were found in patient backgrounds in the JMJD1A-high and JMJD1A-low groups (Table 2). In addition, no significant differences were found in overall survival between groups ($P = 0.6477$; Table 3); the 3-year survival rates of JMJD1A-high and JMJD1A-low groups were 77.8% and 81.6%, respectively (data not shown). However, cancer-related disease-free survival was quite different between groups ($P = 0.0006$, Fig. 2); the 3-year survival rates of JMJD1A-high and JMJD1A-low groups were 63.5% and 88.5%, respectively ($P = 0.0006$; Table 3). Two clinicopathological parameters were also significantly associated with 3-year survival rates: Union for International Cancer Control (UICC) stage ($P = 0.0083$) and microscopic portal vein invasion (PVTT, $P = 0.0380$). However, multivariate Cox regression analysis of these parameters revealed that only JMJD1A expression remained an independent prognostic factor ($P = 0.0016$; hazard ratio = 3.00 [1.54–5.97], Table 3).

Effects of JMJD1A Expression on Growth, Invasion, and EMT in HCC Cells

To assess potential mechanisms of JMJD1A in HCC recurrence, an in vitro knockdown experiment was performed with siRNA in the HCC cell lines, HuH7, PLC, and HepG2. JMJD1A expression was lowest in PLC cells, but the differences among cell lines were not significant (Fig. 3a). Suppression of JMJD1A by siRNA was confirmed with qRT-PCR and Western blotting (Fig. 3b).

To evaluate the effects of hypoxia on HCC cells, we checked growth ability, invasion ability, and expression of EMT-related genes. As described previously, hypoxia reduced proliferation, increased invasive activity, and increased expression of EMT-related genes (Fig. 3c–e).[38,39]

Next, we evaluated the effect of suppressing JMJD1A in hypoxic and normoxic conditions.

After 72 h of treatment, hypoxia-induced growth inhibition was reduced with JMJD1A suppression (Fig. 3c); for example, in the HuH7 cell line, hypoxia inhibited proliferation by 15.5 ± 0.6% ($P = 0.047$); this was reduced to 2.4 ± 0.4% inhibition with hypoxia after JMJD1A siRNA treatment ($P < 0.01$). Similar effects were observed in the HepG2 and PLC cell lines (data not shown).

Additionally, in HuH7 cells, hypoxia stimulated invasion by 5.60 ± 0.1-fold ($P < 0.001$; Fig. 3d); however, this was reduced to only 2.93 ± 0.1-fold stimulation when JMJD1A was suppressed with siRNA treatment. Similar effects were observed in the other cell lines (data not shown). Therefore, siRNA treatment significantly reduced cell invasion stimulated by hypoxic conditions ($P < 0.01$).

EMT was evaluated by quantifying the expression of representative EMT-related mRNAs, including E-cadherin, N-cadherin, and Twist, by qRT-PCR (Fig. 3e). E-cadherin mRNA was expressed in all three cell lines, but N-cadherin and Twist mRNA were expressed at very low or undetectable levels. Hypoxic conditions caused a significant reduction in E-cadherin expression and overexpression of both N-cadherin and Twist in all cell lines. JMJD1A suppression with siRNA apparently reduced E-cadherin expression under normoxic conditions; however, under hypoxic conditions, JMJD1A suppression blocked the effects of hypoxia on E-cadherin, N-cadherin, and Twist mRNA expression.

DISCUSSION

In a preliminary study, we identified several molecular markers that could predict poor prognosis in patients with HCC.[40] Furthermore, we performed transcriptome analysis to explore new molecular indicators.[41–43] However, those insights were not directly related to hypoxia-inducible genes, which are thought to confer malignant potential in other cancers.

For this reason, we compared our previously identified hypoxia-inducible genes with microarray data derived from three HCC cell lines exposed to hypoxic conditions.[25] We found high mRNA levels for 26 genes (data not shown); of those, vascular epithelial growth factor ranked 3rd, egg-laying-defective nine homolog 3 ranked 5th, adrenomedullin ranked 21st, and JMJD1A ranked 9th. All had previously been reported to be poor prognostic factors for human malignancies.[25,44–46] Next, we performed a pilot study using previously published microarray data that represented 139 HCC samples (from patients not included

TABLE 2 Univariate analysis of patient characteristics and JMJD1A mRNA expression

Variable	JMJD1A mRNA expression		*P*-value
	Low ($n = 63$)	High ($n = 47$)	
Age (<65 years:65≤)	30:33	22:25	0.9329
Sex (male:female)	47:16	42:5	0.0844
HBV infection (negative:positive)	50:13	36:11	0.7284
HCV infection (negative:positive)	26:37	20:27	0.8926
Child–Pugh (A:B)	54:9	44:3	0.1766
AFP (<400 ng/ml:400≤)	50:13	33:14	0.2717
PIVKA-II (<40 mAU/m: 40≤)	59:4	45:2	0.6283
Preoperative TACE (yes:no)	35:28	28:19	0.6732
Tumor size (<3 cm:3≤)	19:44	13:34	0.7750
Tumor number (single:multiple)	22:41	16:31	0.9237
Macroscopic PVTT (absent:present)	53:10	32:15	0.0654
Macroscopic IM (absent:present)	43:20	31:16	0.7997
CLIP score (0 or 1:2<)	28:35	18:29	0.5174
JIS (0–2:3<)	46:17	31:16	0.4253
UICC stage (I or II:III or IV)	39:24	26:21	0.4874
Edmondson (I or II:III or IV)	31:32	21:26	0.6380
Microscopic PVTT (absent:present)	45:18	27:20	0.1279
Microscopic IM (absent:present)	50:13	34:13	0.3910
Background of the liver (NL or CH:LC)	37:26	26:21	0.7206

HBV hepatitis B virus, *HCV* hepatitis C virus, *AFP* α-fetoprotein, *PIVKA-II* protein induced by vitamin K absence or antagonist II, *TACE* transarterial chemoembolization, *PVTT* portal vein tumor thrombosis, *IM* intrahepatic metastasis, *CLIP* Cancer of the Liver Italian Program score, *JIS* Japan Integrated Staging, *UICC* Union for International Cancer Control, *NL* normal liver, *CH* chronic hepatitis, *LC* liver cirrhosis

TABLE 3 Univariate and multivariate analyses of disease-free survival

			Univariate	Multivariate	
	n	3-year DFS (%)	*P*-value	HR (95% CI)	*P*-value
Age (<65 years:65≤)	52:57	84.0:71.8	0.2010		
Sex (male:female)	89:21	75.8:86.2	0.6689		
HBV infection (negative:positive)	86:24	76.1:83.6	0.3393		
HCV infection (negative:positive)	46:64	83.2:74.6	0.0977		
Child–Pugh (A:B)	98:12	77.1:85.7	0.1716		
AFP (<400 ng/ml:400≤)	83:27	80.2:68.7	0.4958		
PIVKA-II (<40 mAU/ml:40≤)	104:6	77.5:100	0.4438		
Preoperative TACE (yes:no)	63:47	76.8:79.6	0.8302		
Tumor size (<3 cm:3≤)	32:78	83.4:75.9	0.1474		
Tumor number (single:multiple)	38:72	82.9:64.3	0.1273		
Macroscopic PVTT (absent:present)	85:25	80.8:67.5	0.1855		
Macroscopic IM (absent:present)	74:36	82.9:61.1	0.1167		
CLIP score (0 or 1:2<)	46:74	84.5:72.4	0.1418		
JIS (0–2:3<)	77:33	86.5:51.7	0.1045		
UICC stage (I or II:III or IV)	65:45	86.6:60.4	**0.0083**	2.1127 (0.967–4.098)	0.0517
Edmondson (I or II:III or IV)	52:58	82.6:74.1	0.8658		
Microscopic PVTT (absent:present)	72:38	86.4:47.9	**0.0380**	0.7813 (0.656–2.986)	0.3768
Microscopic IM (absent:present)	84:26	77.4:79.0	0.3984		
Background of the liver (NL or CH:LC)	63:47	78.5:76.9	0.7272		
JMJD1A (low:high)	63:47	88.5:63.5	**0.0006**	2.9984 (1.54–5.97)	**0.0016**

PVTT portal vein tumor thrombosis, *JIS* Japan Integrated Staging, *CLIP* Cancer of the Liver Italian Program score, *CH* chronic hepatitis, *LC* liver cirrhosis, *NL* normal liver, *DFS* disease-free survival

P-value < 0.05 was considered statistically significant, and *bold* indicates significant differences

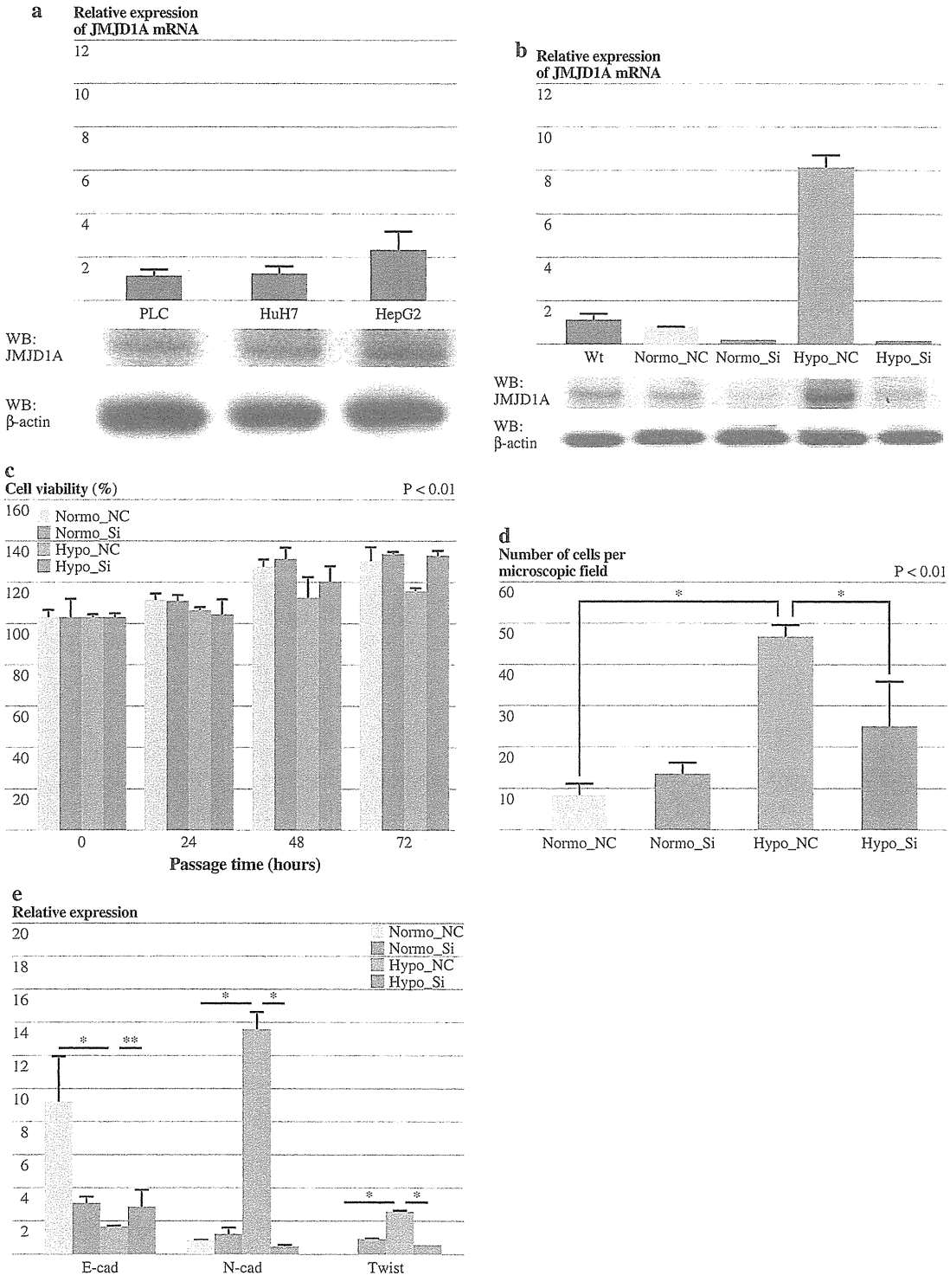

in the series reported herein).[43] We checked those four genes (vascular epithelial growth factor, egg-laying-defective nine homolog 3, adrenomedullin, and JMJD1A) to determine the relationship between expression level and prognosis using these microarray data; there, JMJD1A was the only significant prognostic marker for HCC ($P = 0.0234$, data not shown).

Based on the above preliminary data, in this study, we aimed to evaluate the role of JMJD1A expression in HCC. We demonstrated that JMJD1A expression was higher in

◀**FIG. 3** JMJD1A expression, proliferation, invasion, and EMT-related gene expression under hypoxic conditions. **a** JMJD1A mRNA (upper panel) and protein (lower panel) expression in HCC cell lines (PLC, HuH7, and HepG2). Normoxic conditions. The data represent mean ± SD. **b** PLC cells were treated with (Si) or without (NC) RNA interference of JMJD1A under hypoxic (hypo) or normoxic (normo) conditions. JMJD1A mRNA (upper panel) values represent mean ± SD; protein (lower panel) expression was normalized by endogenous β-actin expression. **c** Proliferation analysis (cell viability) of HuH7 cells under normoxia (normo) or hypoxia (hypo), with (Si) or without (NC) RNA interference of JMJD1A expression. The double, wavy line indicates a break in the numbering on the *Y*-axis. The data represent mean ± SD. *Significant difference between the values under the horizontal line. **d** Invasion assay shows the number of invasive HuH7 cells under normoxia (normo) or hypoxia (hypo), with (Si) or without (NC) RNA interference of JMJD1A expression. The data represent mean ± SD. *Significant difference between the values bracketed. **e** Epithelial–mesenchymal transition expression. Expression of representative mRNAs, E-cadherin (E-cad), N-cadherin (N-cad), and Twist was evaluated under normoxia (normo) or hypoxia (hypo), with (Si) or without (NC) RNA interference of JMJD1A expression. The data represent mean ± SD. Significant differences between values under the horizontal lines are indicated. ($*P < 0.01$, $**P = 0.0125$)

HCC tissues than in the corresponding background liver tissues. Furthermore, we found that high JMJD1A expression was a significant factor for predicting HCC recurrence. Finally, we showed that suppressing JMJD1A expression with siRNA treatment reduced the effects of hypoxia on malignant behaviors.

We demonstrated that both mRNA and protein expression were higher in HCC samples than in the corresponding normal liver tissues. Moreover, imuunostaining showed that JMJD1A was localized in both the nucleus and cytoplasm. This was unexpected, because JMJD1A is a histone H3 lysine 9 demethylase that activates transcription; therefore, JMJD1A would be expected to localize to the nucleus. However, according to Okada et al., when spermatids start to elongate, JMJD1A localizes to the cytoplasm and forms distinct foci; these foci persist until spermiogenesis and disappear in mature spermatozoa.[27] Therefore, in some settings, JMJD1A can localize to the cytoplasm. In this study, 26 of 87 specimens were immunohistochemically positive, including 22 samples that had stained only in the cytoplasm. Nevertheless, there was a significant correlation ($P < 0.0001$) between positive staining and JMJD1A mRNA expression. Thus, we concluded that the positive immunohistochemical reactivity represented true positive expression.

JMJD1A expression was significantly lower in noncancerous than in HCC samples. This suggested that JMJD1A was a potential marker for resected HCC. (Note that, because the JMJD1A-positive lesion might be variable in the tissue depending on relative hypoxia or other tumor-related reasons, this should be evaluated not in biopsy samples but in resected HCC samples.) Furthermore, hypoxia is thought to be induced by TACE in HCC tissue. Nonetheless, there was no significant change in JMJD1A expression with preoperative TACE. That suggested that JMJD1A expression was not only influenced by hypoxic conditions initiated by TACE. This is consistent with the fact that pulmonary metastasis after hepatic artery occlusion occurred only in some cases. In our hands, three HCC cell lines cultured under hypoxic conditions in vitro showed increases in JMJD1A mRNA expression that reached maximum levels (3- to 6-fold) after 48–72 h (data not shown).

Our finding that high JMJD1A expression was significantly associated with HCC recurrence gave rise to the notion that JMJD1A may play a significant role in the malignant transformation of HCC. Although JMJD1A was not significantly associated with overall survival, it was associated with disease-free survival. Several authors mentioned that the prognostic factors for survival after resection were not always coincident with those for HCC recurrence, and furthermore overall survival would be mainly related to vascular invasion and liver function.[47–49] Thus, our results are not in conflict with the consensus.

We also found that siRNA suppression of JMJD1A caused a reduction in hypoxia-induced cellular invasion. Our results suggested that this reduction was due to inhibition of EMT. Although no studies have indicated that JMJD1A could lead to EMT in other cancers, it was reported that JMJD1A positively regulated the expression of pluripotency-associated genes in embryonic stem cells, which self-renew indefinitely.[50,51] Moreover, in JMJD1A-deficient mice, mesenchymal tissues primarily developed into fat tissue in adults.[52] Taken together, the evidence suggests that JMJD1A may maintain the undifferentiated state, particularly in mesenchymal stem cells; thus, we hypothesized that, in epithelial cancer, such as HCC, JMJD1A expression may induce EMT. In the present study, our results on invasion and EMT expression were consistent with that hypothesis. Also, in proliferation assay, suppression of JMJD1A caused a decrease in the growth inhibition under hypoxic conditions. In hypoxic conditions, cells exhibit various behaviors to survive, and hypoxia-inducible genes play a critical role in eliciting cellular responses; for example, they may induce cell cycle arrest or apoptosis in irreversibly damaged cells.[53,54] Our data suggested that suppressing JMJD1A did not cause these cellular responses under hypoxic conditions.

In summary, our results suggest that JMJD1A is a sensitive recurrence marker, and JMJD1A can promote malignant transformation via EMT. Moreover, JMJD1A could be a promising therapeutic target for treating HCC.

CONFLICT OF INTEREST The authors declare no conflict of interest.

REFERENCES

1. Llovet JM, Burroughs A, Bruix J. Hepatocellular carcinoma. *Lancet.* 2003;362:1907–17.
2. Nagano H, Miyamoto A, Wada H, et al. Interferon-alpha and 5-fluorouracil combination therapy after palliative hepatic resection in patients with advanced hepatocellular carcinoma, portal venous tumor thrombus in the major trunk, and multiple nodules. *Cancer.* 2007;110:2493–501.
3. Nagano H. Treatment of advanced hepatocellular carcinoma: intraarterial infusion chemotherapy combined with interferon. *Oncology.* 2010;78 Suppl 1:142–7.
4. Murakami M, Nagano H, Kobayashi S, et al. The beneficial effect of preoperative transcatheter arterial chemoembolization for resectable hepatocellular carcinoma: Implication of circulating cancer cells detecting alpha-fetoprotein mRNA. *Mol Therapeut Med.* 2010;1:485–91.
5. Llovet JM, Bruix J. Molecular targeted therapies in hepatocellular carcinoma. *Hepatology.* 2008;48:1312–27.
6. Liou TC, Shih SC, Kao CR, Chou SY, Lin SC, Wang HY. Pulmonary metastasis of hepatocellular carcinoma associated with transarterial chemoembolization. *J Hepatol.* 1995;23:563–8.
7. Song BC, Chung YH, Kim JA, et al. Association between insulin-like growth factor-2 and metastases after transcatheter arterial chemoembolization in patients with hepatocellular carcinoma: a prospective study. *Cancer.* 2001;91:2386–93.
8. Ebos JM, Lee CR, Cruz-Munoz W, Bjarnason GA, Christensen JG, Kerbel RS. Accelerated metastasis after short-term treatment with a potent inhibitor of tumor angiogenesis. *Cancer Cell.* 2009;15:232–9.
9. Paez-Ribes M, Allen E, Hudock J, et al. Antiangiogenic therapy elicits malignant progression of tumors to increased local invasion and distant metastasis. *Cancer Cell.* 2009;15:220–31.
10. Semenza GL. Hypoxia and cancer. *Cancer Metastasis Rev.* 2007;26:223–4.
11. Colpaert C, Vermeulen P, van Beest P, et al. Intratumoral hypoxia resulting in the presence of a fibrotic focus is an independent predictor of early distant relapse in lymph node-negative breast cancer patients. *Histopathology.* 2001;39:416–25.
12. Koukourakis MI, Giatromanolaki A, Sivridis E, et al. Hypoxia-regulated carbonic anhydrase-9 (CA9) relates to poor vascularization and resistance of squamous cell head and neck cancer to chemoradiotherapy. *Clin Cancer Res.* 2001;7:3399–403.
13. Giatromanolaki A, Koukourakis MI, Sivridis E, et al. Expression of hypoxia-inducible carbonic anhydrase-9 relates to angiogenic pathways and independently to poor outcome in non-small cell lung cancer. *Cancer Res.* 2001;61:7992–8.
14. Fyles A, Milosevic M, Hedley D, et al. Tumor hypoxia has independent predictor impact only in patients with node-negative cervix cancer. *J Clin Oncol.* 2002;20:680–7.
15. Vaupel P, Mayer A. Hypoxia in cancer: significance and impact on clinical outcome. *Cancer Metastasis Rev.* 2007;26:225–39.
16. Wada H, Nagano H, Yamamoto H, et al. Expression pattern of angiogenic factors and prognosis after hepatic resection in hepatocellular carcinoma: importance of angiopoietin-2 and hypoxia-induced factor-1 alpha. *Liver Int.* 2006;26:414–23.
17. Graeber TG, Osmanian C, Jacks T, et al. Hypoxia-mediated selection of cells with diminished apoptotic potential in solid tumours. *Nature.* 1996;379:88–91.
18. Gupta S, Kobayashi S, Phongkitkarun S, Broemeling LD, Kan Z. Effect of transcatheter hepatic arterial embolization on angiogenesis in an animal model. *Invest Radiol.* 2006;41:516–21.
19. Li X, Feng GS, Zheng CS, Zhuo CK, Liu X. Influence of transarterial chemoembolization on angiogenesis and expression of vascular endothelial growth factor and basic fibroblast growth factor in rat with Walker-256 transplanted hepatoma: an experimental study. *World J Gastroenterol.* 2003;9:2445–9.
20. Liao XF, Yi JL, Li XR, Deng W, Yang ZF, Tian G. Angiogenesis in rabbit hepatic tumor after transcatheter arterial embolization. *World J Gastroenterol.* 2004;10:1885–9.
21. Forsythe JA, Jiang BH, Iyer NV, et al. Activation of vascular endothelial growth factor gene transcription by hypoxia-inducible factor 1. *Mol Cell Biol.* 1996;16:4604–13.
22. Chi JT, Wang Z, Nuyten DS, et al. Gene expression programs in response to hypoxia: cell type specificity and prognostic significance in human cancers. *PLoS Med.* 2006;3:e47.
23. Brahimi-Horn MC, Chiche J, Pouyssegur J. Hypoxia and cancer. *J Mol Med.* 2007;85:1301–7.
24. van Malenstein H, Gevaert O, Libbrecht L, et al. A seven-gene set associated with chronic hypoxia of prognostic importance in hepatocellular carcinoma. *Clin Cancer Res.* 2010;16:4278–88.
25. Uemura M, Yamamoto H, Takemasa I, et al. JMJD1A is a novel prognostic marker for colorectal cancer; Identification from in vivo hypoxic tumor cells. *Clin Cancer Res.* 2010;18:4636–46.
26. Arun C, London NJ, Hemingway DM. Prognostic significance of elevated endothelin-1 levels in patients with colorectal cancer. *Int J Biol Markers.* 2004;19:32–7.
27. Okada Y, Scott G, Ray MK, Mishina Y, Zhang Y. Histone demethylase JHDM2A is critical for Tnp1 and Prm1 transcription and spermatogenesis. *Nature.* 2007;450:119–23.
28. Yamane K, Toumazou C, Tsukada Y, et al. JHDM2A, a JmjC-containing H3K9 demethylase, facilitates transcription activation by androgen receptor. *Cell.* 2006;125:483–95.
29. Adam K, Erinn R, Denise C, Olga R, Sully F, Amato G. Regulation of the histone demethylase JMJD1A by hypoxia-inducible factor 1 enhances hypoxic gene expression and tumor growth. *Mol Cell Biol.* 2010;30:344–53.
30. Hayashi N, Yamamoto H, Hiraoka N, et al. Differential expression of cyclooxygenase-2 (COX-2) in human bile duct epithelial cells and bile duct neoplasm. *Hepatology.* 2001;34:638–50.
31. Yamamoto H, Kondo M, Nakamori S, et al. JTE-522, a cyclooxygenase-2 inhibitor, is an effective chemopreventive agent against rat experimental liver fibrosis1. *Gastroenterology.* 2003;125:556–71.
32. Yang MH, Chen CL, Chau GY, et al. Comprehensive analysis of the independent effect of twist and snail in promoting metastasis of hepatocellular carcinoma. *Hepatology.* 2009;50:1464–74.
33. Ning B, Ding J, Yin C, et al. Hepatocyte nuclear factor 4 alpha suppresses the development of hepatocellular carcinoma. *Cancer Res.* 2010;70:7640–51.
34. Ding ZB, Shi YH, Zhou J, et al. Liver-intestine cadherin predicts microvascular invasion and poor prognosis of hepatitis B virus-positive hepatocellular carcinoma. *Cancer.* 2009;115:4753–65.
35. Shiokawa T, Hattori Y, Kawano K, et al. Effect of polyethylene glycol linker chain length of folate-linked microemulsions loading aclacinomycin A on targeting ability and antitumor effect in vitro and in vivo. *Clin Cancer Res.* 2005;11:2018–25.
36. Seton-Rogers SE, Lu Y, Hines LM, et al. Cooperation of the ErbB2 receptor and transforming growth factor beta in induction of migration and invasion in mammary epithelial cells. *Proc Natl Acad Sci U S A.* 2004;101:1257–62.
37. Youden WJ. Index for rating diagnostic tests. *Cancer.* 1950;3:32–5.
38. Yang MH, Wu MZ, Chiou SH, et al. Direct regulation of TWIST by HIF-1alpha promotes metastasis. *Nat Cell Biol.* 2008;10:295–305.
39. Liu L, Ren ZG, Shen Y, et al. Influence of hepatic artery occlusion on tumor growth and metastatic potential in a human

orthotopic hepatoma nude mouse model: relevance of epithelial-mesenchymal transition. *Cancer Sci.* 2009;101:120–8.
40. Damdinsuren B, Nagano H, Kondo M, et al. TGF-beta1-induced cell growth arrest and partial differentiation is related to the suppression of Id1 in human hepatoma cells. *Oncol Rep.* 2006;15:401–8.
41. Kittaka N, Takemasa I, Seno S, et al. Exploration of potential genomic portraits associated with intrahepatic recurrence in human hepatocellular carcinoma. *Ann Surg Oncol.* 2010;17:3145–54.
42. Kurokawa Y, Honma K, Takemasa I, et al. Central genetic alterations common to all HCV-positive, HBV-positive and non-B, non-C hepatocellular carcinoma: a new approach to identify novel tumor markers. *Int J Oncol.* 2006;28:383–91.
43. Yoshioka S, Takemasa I, Nagano H, et al. Molecular prediction of early recurrence after resection of hepatocellular carcinoma. *Eur J Cancer.* 2009;45:881–9.
44. Ishigami SI, Arii S, Furutani M, et al. Predictive value of vascular endothelial growth factor (VEGF) in metastasis and prognosis of human colorectal cancer. *Br J Cancer.* 1998;78:1379–84.
45. Couvelard A, Deschamps L, Rebours V, et al. Overexpression of the oxygen sensors PHD-1, PHD-2, PHD-3, and FIH Is associated with tumor aggressiveness in pancreatic endocrine tumors. *Clin Cancer Res.* 2008;14:6634–9.
46. Hata K, Takebayashi Y, Akiba S, et al. Expression of the adrenomedullin gene in epithelial ovarian cancer. *Mol Hum Reprod.* 2000;6:867–72.
47. Poon RT, Ng IO, Fan ST, et al. Clinicopathologic features of long-term survivors and disease-free survivors after resection of hepatocellular carcinoma: a study of a prospective cohort. *J Clin Oncol.* 2001;19:3037–44.
48. Arii S, Tanaka J, Yamazoe Y, et al. Predictive factors for intrahepatic recurrence of hepatocellular carcinoma after partial hepatectomy. *Cancer.* 1992:69:913–9.
49. The Japan Society of Hepatology. Clinical Practice Guidelines for Hepatocellular Carcinoma - The Japan Society of Hepatology 2009 update. *Hepatol Res.* 2010;40:2–144.
50. McGraw S, Vigneault C, Sirard MA. Temporal expression of factors involved in chromatin remodeling and in gene regulation during early bovine in vitro embryo development. *Reproduction.* 2007;133:597–608.
51. Loh YH, Zhang W, Chen X, George J, Ng HH. Jmjd1a and Jmjd2c histone H3 Lys 9 demethylases regulate self-renewal in embryonic stem cells. *Genes Dev.* 2007;21:2545–57.
52. Inagaki T, Tachibana M, Magoori K, et al. Obesity and metabolic syndrome in histone demethylase JHDM2a-deficient mice. *Genes Cells.* 2009;14:991–1001.
53. Semenza GL. Targeting HIF-1 for cancer therapy. *Nat Rev Cancer.* 2003;3:721–32.
54. Simon MC, Keith B. The role of oxygen availability in embryonic development and stem cell function. *Nat Rev Mol Cell Biol.* 2008;9:285–96.

ErbB receptor tyrosine kinase/NF-κB signaling controls mammosphere formation in human breast cancer

Kunihiko Hinohara[a], Seiichiro Kobayashi[b], Hajime Kanauchi[c], Seiichiro Shimizu[d], Kotoe Nishioka[e], Ei-ichi Tsuji[e], Kei-ichiro Tada[e], Kazuo Umezawa[f], Masaki Mori[g], Toshihisa Ogawa[e], Jun-ichiro Inoue[h], Arinobu Tojo[b], and Noriko Gotoh[a,1]

[a]Division of Systems Biomedical Technology, Institute of Medical Science, University of Tokyo, Minato-ku, Tokyo 108-8639, Japan; [b]Division of Molecular Therapy, Advanced Clinical Research Center, Institute of Medical Science, University of Tokyo, Minato-ku, Tokyo 108-8639, Japan; [c]Department of Breast and Endocrine Surgery, Showa General Hospital, Kodaira-shi, Tokyo 187-8510, Japan; [d]Department of Pathological Diagnosis, Showa General Hospital, Kodaira-shi, Tokyo 187-8510, Japan; [e]Department of Breast and Endocrine Surgery, Graduate School of Medicine, University of Tokyo, Bunkyo-ku, Tokyo 113-8655, Japan; [f]Department of Applied Chemistry, Faculty of Science and Technology, Keio University, Yokohama-shi, Kanagawa 223-8522, Japan; [g]Department of Gastroenterological Surgery, Osaka University, Suita-shi, Osaka, 565-0871, Japan; [h]Division of Cellular and Molecular Biology, Institute of Medical Science, University of Tokyo, Minato-ku, Tokyo 108-8639, Japan

Edited by Joseph Schlessinger, Yale University School of Medicine, New Haven, CT, and approved March 8, 2012 (received for review August 15, 2011)

Breast cancer is one of the most common cancers in humans. However, our understanding of the cellular and molecular mechanisms underlying tumorigenesis in breast tissues is limited. Here, we identified a molecular mechanism that controls the ability of breast cancer cells to form multicellular spheroids (mammospheres). We found that heregulin (HRG), a ligand for ErbB3, induced mammosphere formation of a breast cancer stem cell (BCSC)–enriched population as well as in breast cancer cell lines. HRG-induced mammosphere formation was reduced by treatment with inhibitors for phosphatidyl inositol 3-kinase (PI3K) or NF-κB and by expression of IκBα-Super Repressor (IκBαSR), a dominant-negative inhibitor for NF-κB. Moreover, the overexpression of IκBαSR in breast cancer cells inhibited tumorigenesis in NOD/SCID mice. Furthermore, we found that the expression of IL8, a regulator of self-renewal in BCSC-enriched populations, was induced by HRG through the activation of the PI3K/NF-κB pathway. These findings illustrate that HRG/ErbB3 signaling appears to maintain mammosphere formation through a PI3K/NF-κB pathway in human breast cancer.

EGF | HER | tumor sphere | cancer stem cells | inflammation

Cancer stem cells (CSCs), which make up only a small proportion of heterogeneous tumor cells, may possess a greater ability to maintain tumorigenesis than other tumor cell types (1, 2). CSCs can self-renew and simultaneously produce differentiated daughter cells; thus they can strongly proliferate until they reach their final differentiated state. With improvements in the isolation of CSCs, there is now a growing body of evidence that, in some cases of hematologic and solid tumors, a cancer stem cell population can be enriched based on phenotype (3–10). In human breast cancers, breast cancer stem cells (BCSCs) are enriched in the $CD44^{high}/CD24^{low}$ cell population, whereas the $CD44^{low}/CD24^{high}$ cells represent a more differentiated phenotype with limited stem cell–like potential (3). Because BCSCs withstand anoikis in culture, they expand under anchorage-independent conditions, giving rise to clonal spheroids (mammospheres), which can be serially passaged in vitro (11, 12). These processes can in part recapitulate the breast tumorigenesis process (13–16). To develop more effective cancer therapies, it would be reasonable to target molecules that have a critical role in the maintenance of mammospheres. However, the molecular mechanism by which mammospheres are maintained is still largely obscure.

NF-κB is a transcription factor complex that is typically a heterodimer of p50, p52, p65 (RelA), RelB, and c-Rel. It is usually inactive and bound to IκB, an inhibitory protein, in the cytoplasm. The primary mechanism of regulation of NF-κB activity is through activation of the IKK complex, including heterodimers of IKKα and IKKβ, as a result of various signaling pathways. The serine–threonine kinase Akt is one of the activators of IKKβ (17), and the activated IKK complex phosphorylates the IκBα protein, resulting in its ubiquitination, proteasome-mediated degradation, and subsequent release of NF-κB for nuclear translocation. Released NF-κB translocates to the nucleus and binds to the κB sequence, where it promotes the transcription of various genes, including inflammatory chemokines. Recently, we found activation of inflammatory signaling pathways in association with an increase in NF-κB activity in BCSC-enriched populations (18, 19). However, the role of NF-κB and the molecular mechanisms by which NF-κB is activated during mammosphere formation remain unknown.

Heregulin (HRG, also called neuregulin) is a ligand for ErbB3, which is one of the four members of the EGF receptor ErbB family (20). Expression of HRG in the mammary gland induces adenocarcinomas in animal models (21) and favors metastatic spread of breast cancer cells (22). HRG is expressed in 30% of human breast cancer patients (23) and correlates with poor histological grade (24). Recently, it was reported that ErbB2 overexpression increases the stem/progenitor cell population of both normal and malignant mammary cells (25); however the role of HRG and ErbB3 in regulating the properties of BCSC-enriched populations remains largely unknown.

In the present study, we showed that HRG induced mammosphere formation of cancer cells from a BCSC-enriched population. Moreover, our findings suggest that the activity of phosphatidyl inositol 3-kinase (PI3K)/NF-κB is essential for the HRG-induced mammosphere formation.

Results

HRG Induces Mammosphere Formation of a BCSC-Enriched Population. To test the mammosphere-forming ability of a BCSC-enriched population, we initially isolated $CD44^{high}/CD24^{low}/lineage^-$ BCSC-enriched population and $CD44^{low}/CD24^{high}/lineage^-$ nonstem cells from human breast cancer tissue. When these cells were cultured with conventional mammosphere culture media containing EGF, bFGF, and B27 supplement (13, 26), the $CD44^{high}/CD24^{low}/lineage^-$ BCSC-enriched population generated mammospheres, whereas the $CD44^{low}/CD24^{high}/lineage^-$ nonstem cells did not form mammospheres (Fig. 1 *A* and *B*). These observations suggest that cells with the capacity to

Author contributions: K.H. and N.G. designed research; K.H. performed research; S.K., H.K., S.S., K.N., E.-i.T., K.-i.T., K.U., M.M., T.O., J.-i.I., and A.T. contributed new reagents/analytic tools; K.H. analyzed data; and K.H. and N.G. wrote the paper.

The authors declare no conflict of interest.

This article is a PNAS Direct Submission.

Freely available online through the PNAS open access option.

[1]To whom correspondence should be addressed. E-mail: ngotoh@ims.u-tokyo.ac.jp

This article contains supporting information online at www.pnas.org/lookup/suppl/doi:10.1073/pnas.1113271109/-/DCSupplemental.

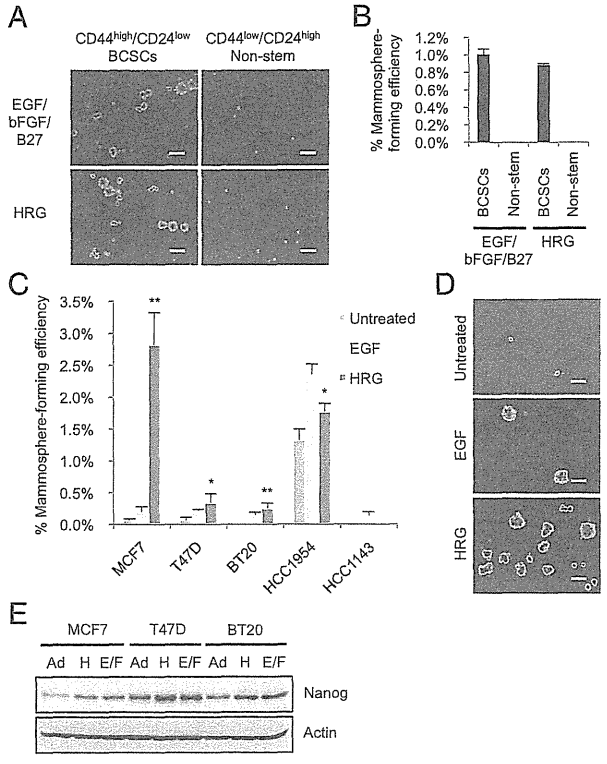

Fig. 1. Effect of HRG on mammosphere formation of a BCSC-enriched population. (*A*) Representative images of primary cultures of mammospheres formed from the sorted $CD44^{high}/CD24^{low}$/lineage$^-$ BCSC-enriched population (*Left*) and the $CD44^{low}/CD24^{high}$/lineage$^-$ nonstem cell population (*Right*) obtained from a specimen of invasive ductal carcinoma (IDC1, Table S1). The cells from IDC1 were incubated with EGF/bFGF/B27 (*Top*) or with 20 ng/mL HRG (*Bottom*). Scale bar = 100 μm. (*B*) The spheres were counted and the percentage of mammosphere-forming cells were determined in each group (data are mean ± SD; $n = 4$). (*C*) Mammosphere assay in MCF7, T47D, BT20, HCC1954, and HCC1143 breast cancer cell lines treated with 20 ng/mL EGF or 20 ng/mL HRG (data are mean ± SD; $n = 4$, $^{**}P < 0.01$, $^{*}P < 0.05$, relative to the values in the respective untreated controls). (*D*) Images showing mammosphere formation in MCF7 cells treated as indicated in (C). Scale bar = 100 μm. (*E*) Nanog protein expression levels in the parental cells growing in 2D adherent (Ad) culture, sphere cells cultured with 20 ng/mL HRG (H) and sphere cells cultured with EGF/bFGF/B27 (E/F).

form mammospheres are enriched in $CD44^{high}/CD24^{low}$/lineage$^-$ cells, confirming that mammospheres can be derived from BCSC-enriched populations as described previously (26, 27).

To examine the effects of HRG on the mammosphere formation, we cultured these cells with HRG in the absence of EGF, bFGF, or B27 supplement and then counted the number of mammospheres that formed. $CD44^{high}/CD24^{low}$/lineage$^-$ BCSC-enriched population cultured with HRG generated mammospheres at similar frequencies as those cultured with EGF/bFGF/B27, whereas $CD44^{low}/CD24^{high}$/lineage$^-$ nonstem cells did not generate mammospheres (Fig. 1 *A* and *B*). These findings suggest that HRG has the ability to induce mammosphere formation of BCSC-enriched population.

To further investigate the effect of HRG, we examined mammosphere formation in five breast cancer cell lines treated with HRG. Similar to the effects of HRG on primary human breast cancer cells, HRG increased mammosphere formation in four of the five breast cancer cell lines (Fig. 1 *C* and *D*) with an efficiency comparable to that of EGF. The HRG-induced mammospheres expressed the stem cell marker Nanog, comparable to mammospheres cultured with EGF/bFGF/B27 (Fig. 1*E*). Together, these results suggest that HRG plays an important role in enhancing the mammosphere formation of BCSC-enriched populations.

HRG Up-Regulates NF-κB Through PI3K/Akt Activation. To examine whether HRG treatment activates the ErbB2/ErbB3 pathway, we investigated the effect of HRG on the phosphorylation levels of ErbB2, ErbB3, ERK, and Akt in three breast cancer cell lines. HRG markedly induced the phosphorylation of ErbB2, ErbB3, ERK, and Akt (Fig. 2*A*) in all three cell lines, suggesting that HRG strongly activates ErbB2 and ErbB3, which leads to the activation of ERK and the PI3K/Akt pathway. To confirm that HRG promotes the interaction between ErbB2 and ErbB3, we performed an immunoprecipitation analysis after treatment with HRG. The analysis revealed that treatment with HRG led to increased interactions between ErbB3 and ErbB2 (Fig. 2*B*).

Because NF-κB is a downstream target of Akt, we investigated whether the NF-κB signaling pathway was also altered by HRG treatment. IKKα/β are the upstream kinases involved in the phosphorylation of IκBα, which leads to the nuclear translocation of NF-κB. Treatment with HRG markedly induced the phosphorylation of Akt and IKKα/β within 10 min and the phosphorylation of IκBα and the NF-κB subunit RELA after 30 min (Fig. 2*C*). To examine the DNA-binding activity of RELA after HRG stimulation, we quantified the intensity of the RELA/DNA complex by ELISA at various time intervals. Treatment with HRG induced a marked increase in the binding activity of RELA after 1 h, and then this activation gradually decreased until 4 h (Fig. 2*D*). To test whether the activation of RELA by HRG was dependent on the PI3K/Akt pathway, we pretreated cells with LY294002, an inhibitor of PI3K before the addition of HRG. As anticipated, the HRG-induced activation of NF-κB was completely inhibited by LY294002 in a manner similar to the inhibition after treatment with DHMEQ, a specific inhibitor of NF-κB (28) (Fig. 2*E* and Fig. S1). These results showed that NF-κB was activated by HRG through the PI3K/Akt pathway. Because our previous observations suggested that the NF-κB pathway is enriched in BCSCs (19), we speculated that the HRG/PI3K/Akt/NF-κB axis may have a role in regulating mammosphere formation.

HRG/PI3K/NF-κB Axis Controls Mammosphere Formation. To elucidate whether NF-κB or PI3K influences HRG-induced mammosphere formation, we treated MCF7 cells with HRG, together with DHMEQ or LY294002. Treatment with DHMEQ or LY294002 decreased the frequency of mammosphere formation in a dose-dependent manner (Fig. 3*A*); however, the sizes of the mammospheres were not significantly changed, suggesting that the activities of NF-κB or PI3K affect mammosphere initiation but do not primarily influence cell proliferation during mammosphere growth. To test secondary mammosphere formation, primary mammospheres generated in the presence of DHMEQ or LY294002 were dissociated into single cells and incubated with HRG in the absence of the inhibitors (Fig. 3*B*). We found that the cells derived from primary mammospheres formed in the presence of DHMEQ or LY294002 did not form secondary mammospheres as efficiently as cells from untreated mammospheres (Fig. 3 *C* and *D*). These findings suggest that the activities of NF-κB and PI3K are required to maintain mammosphere cells with the ability to initiate HRG-induced mammosphere formation. In agreement with these findings, we found that lapatinib, an inhibitor of EGF receptor and ErbB2 tyrosine kinases, decreased NF-κB activity and mammosphere formation (Fig. S2 and *SI Results*). To determine whether DHMEQ or LY294002 induces apoptosis, we stained mammosphere cells with propidium iodide (PI) following inhibitor treatments and then analyzed the cell-cycle status by flow cytometry (Fig. S3). There was no apparent sub-G1 cell population, indicating that

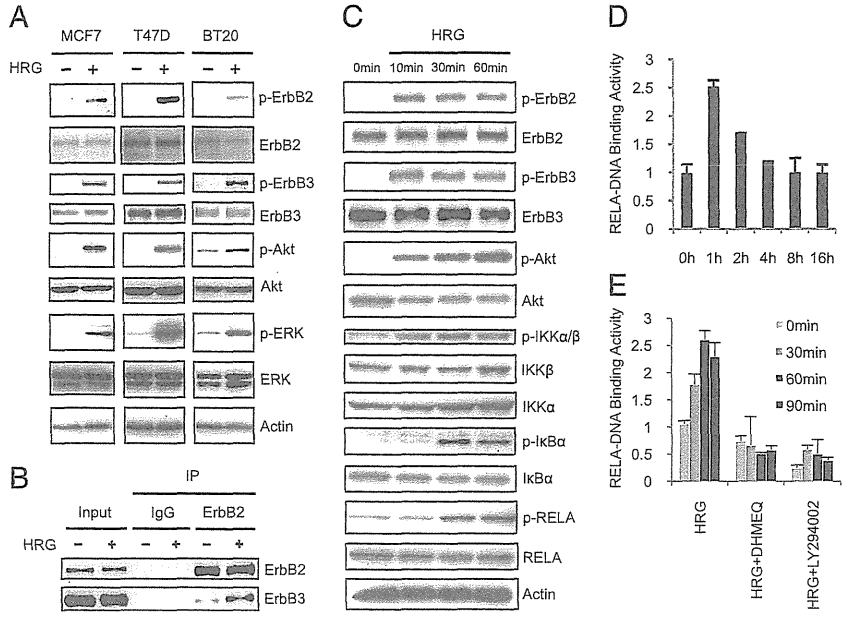

Fig. 2. HRG induces the ErbB/PI3K/Akt/NF-κB pathway. (*A*) MCF7, T47D, and BT20 cells were treated with 100 ng/mL HRG for 10 min, and protein expression levels were determined by immunoblotting. (*B*) MCF7 cells were treated with 100 ng/mL HRG for 10 min, and immunoprecipitation (IP) assays were performed with the indicated antibodies. (*C*) MCF7 cells were treated with 100 ng/mL HRG for 10, 30, and 60 min. Protein expression levels were determined by immunoblotting. (*D*) MCF7 cells were treated with 100 ng/mL HRG for 1, 2, 4, 8, and 16 h. The DNA binding activity of RELA was quantified by ELISA (data are mean ± SD; $n = 3$). (*E*) MCF7 cells were treated with 5 μg/mL DHMEQ (NF-κB inhibitor) or 10 μM LY294002 (PI3Kinase inhibitor) for 2 h, and then the cells were treated with 100 ng/mL HRG for 30, 60, and 90 min. The DNA-binding activity of RELA was quantified by ELISA (data are mean ± SD; $n = 3$).

the inhibitors did not induce apoptosis at the effective concentrations for mammosphere formation.

NF-κB Is Required to Maintain Mammosphere-Forming Ability and Tumorigenic Potential of MCF7 Breast Cancer Cells. To further validate these findings, we overexpressed mutant IκBα (IκBαSR), a dominant-negative inhibitor of NF-κB, in MCF7 cells with a lentiviral vector. Overexpression of mutant IκBα resulted in a decrease in the number of HRG-induced mammospheres compared with the vector-transduced cells (Fig. 3*E*). We also attempted to determine whether NF-κB regulates the mammosphere-forming ability in culture containing EGF/bFGF/B27, and found that NF-κB activity was required for mammosphere formation in such a culture condition. These results suggest that NF-κB is a mediator of mammosphere-forming capacity in both HRG- and EGF/bFGF/B27-containing media (Figs. S4 and S5 and *SI Results*).

To test whether the down-regulation of NF-κB signaling alters the tumor-initiating ability in vivo, we injected 1×10^5 MCF7 cells constitutively expressing mutant IκBα into the mammary fat pads of NOD/SCID mice. There were no significant morphological differences between these cells and control cells in culture (Fig. S6, *Upper*). All eight mice injected with control cells developed tumors within 6 wk, whereas tumor formation was inefficient in the mice injected with cells expressing mutant IκBα (four of eight mice) (Fig. 3*F*). Histological analysis showed that tumors derived from the vector-transduced cells or IκBαSR-transduced cells had a similar morphology (Fig. S6, *Lower*). Therefore, it is unlikely that the reduced incidence of tumor formation by expression of IκBαSR is due to cell differentiation; rather, it appears that NF-κB activity is required for tumor initiation of MCF7 cells in vivo.

By extension, we speculated that an NF-κB-negative subpopulation could not generate mammospheres. To isolate living cells based on NF-κB activity, we used an NF-κB reporter lentiviral vector expressing d2Venus (a yellow fluorescent protein) driven by four copies of the NF-κB response element located upstream of the minimal TATA promoter. We isolated MCF7 cells expressing d2Venus at high ($NFkB^+$) or low ($NFkB^-$) levels (Fig. 3*G*); the activity of NF-κB is thought to be higher in the former cells than in the latter cells. As expected, the NF-κB–negative subpopulation showed significantly decreased mammosphere formation capacity compared with the NF-κB–positive subpopulation (Fig. 3*H*). Taken together, these in vitro and in vivo results showed that NF-κB is required for mammosphere formation and tumor initiation of MCF7 cells.

HRG Elicits PI3K/NF-κB–Dependent Up-Regulation of IL8 mRNA Expression. IL8 signaling has been shown to play a role in BCSC self-renewal (29, 30). Because the expression of *IL8* is regulated by NF-κB activity (31), we investigated whether HRG induces the expression of *IL8*. We also examined the expression of representative immediate early genes, *c-Fos* and *c-Myc*. Treatment with HRG resulted in a dramatic increase of *IL8* expression (up to a 100-fold increase) after 2 h (Fig. 4 *A* and *B*). The expression levels of *c-Fos* and *c-Myc* were also increased (10-fold and five-fold, respectively) (Fig. 4 *A* and *B*). The levels of these mRNAs were decreased rapidly after 4 h. To determine whether the activity of NF-κB or PI3K is involved in the induction of *IL8* expression by HRG, cells were stimulated with HRG in the presence of DHMEQ or LY294002. We found that the levels of *IL8* induction by HRG were decreased by treatment with inhibitors, although the induction levels of *c-Fos* or *c-Myc* were not significantly changed (Fig. 4 *A* and *B*). These results suggest that the expression of *IL8* is induced by the HRG/PI3K/NF-κB axis.

HRG/PI3K/NF-κB Axis Controls Mammosphere Formation of Primary Tumor Cells Derived from Breast Cancer Patients. We extended our analyses to primary tumor cells isolated directly from human breast cancer tissues (Table S1). To assess the effect of HRG,

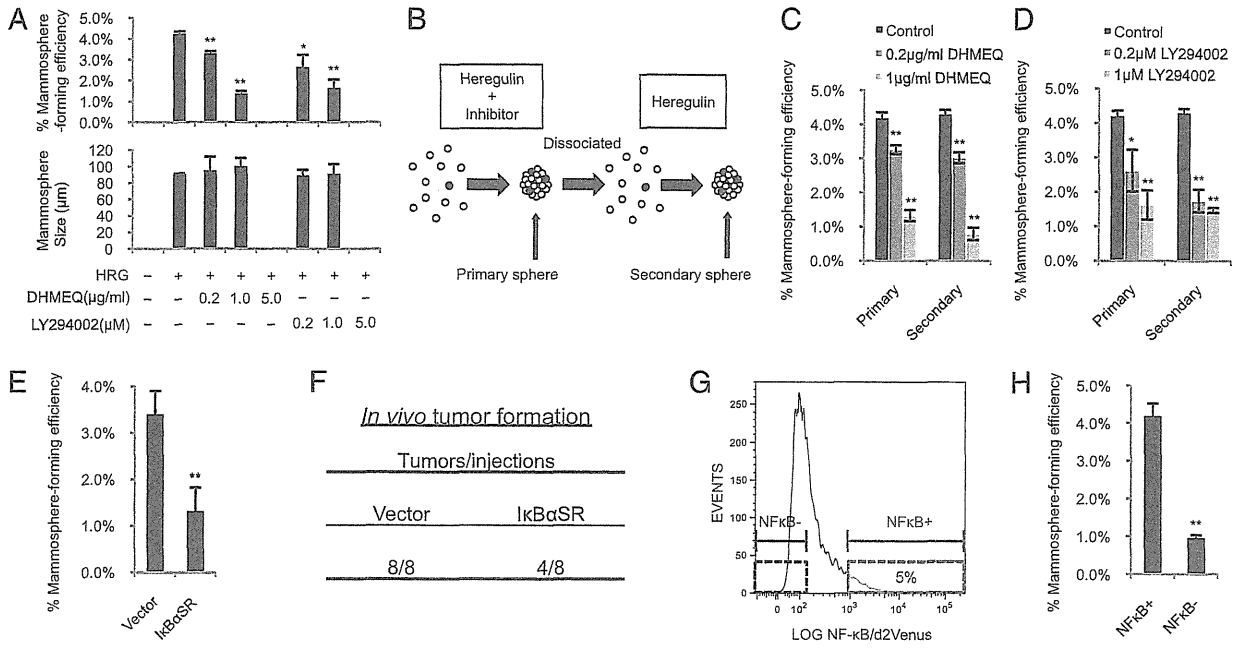

Fig. 3. Role of the HRG/PI3K/NF-κB axis on mammosphere formation. (*A*) MCF7 cells were incubated with 20 ng/mL HRG and/or the indicated concentrations of DHMEQ and LY294002. The number of formed mammospheres was counted, and the percentage of mammosphere-forming cells was determined [data are mean ± SD; $n = 3$, $^{**}P < 0.01$, $^{*}P < 0.05$, relative to the values in the HRG(+)]. (*B*) Experimental strategies for evaluating the effect of initial treatment with inhibitors on secondary mammosphere formation. (*C* and *D*) Effects of DHMEQ and LY294002 on primary and secondary mammosphere formation. MCF7 cells were incubated with 20 ng/mL HRG and/or the indicated concentrations of DHMEQ and LY294002. The formed primary mammospheres were dissociated into single cells and grown as secondary mammospheres without treatment with inhibitors. The mammospheres were counted, and the percentage of mammosphere-forming cells was determined (data are mean ± SD; $n = 3$, $^{**}P < 0.01$, $^{*}P < 0.05$, relative to the values in the respective controls). (*E*) MCF7 cells expressing the indicated lentiviral vectors were incubated with 20 ng/mL HRG, and the percentage of mammosphere-forming cells was determined (data are mean ± SD; $n = 4$, $^{**}P < 0.01$). (*F*) NOD/SCID mice were injected in the mammary fat pad with 1×10^5 of vector- or IκBαSR-transduced MCF7 cells. Tumor formation was indicated by tumors/injections at 6 wk after injection. (*G*) NF-κB reporter activity of mammospheres derived from MCF7 cells. (*H*) NF-κB$^+$ cells and NF-κB$^-$ cells (Fig. 3*G*) were sorted by FACS and cultured with 20 ng/mL HRG. The percentage of mammosphere-forming cells was determined (data are mean ± SD; $n = 4$, $^{**}P < 0.01$).

PI3K, and NF-κB on mammosphere formation, primary tumor cells were treated with HRG, together with DHMEQ or LY294002. Treatment with HRG induced mammosphere formation in all tumor samples, and the effect of HRG was blocked when DHMEQ or LY294002 was added with HRG (Fig. 5*A* and *B*). We confirmed that both ErbB2 and ErbB3 were expressed in these cells and that the phosphorylation of Akt and IκBα was induced in response to HRG (Fig. 5*C*). When we treated primary tumor cells with HRG, together with LY294002, the phosphorylation levels of Akt and IκBα were decreased, suggesting that NF-κB was activated by HRG through the PI3K/Akt pathway in primary tumor cells. (Fig. S1). Furthermore, overexpression of mutant IκBα in primary tumors cells with a lentiviral vector led to a decreased frequency of mammosphere formation compared with the control vector–transduced cells (Fig. 5*D*). Similar results were obtained in mammospheres cultured with EGF/bFGF/B27 (Fig. 5*D* and Fig. S7 *A* and *B*). These results suggest that the mammosphere formation of primary tumor cells derived from breast cancer patients is regulated by the HRG/PI3K/NF-κB pathway, which is consistent with the results obtained from the analysis performed with breast cancer cell lines.

Discussion

Accumulating evidence indicates that BCSCs are responsible for the initiation, propagation, recurrence, and radioresistance of breast cancers (1, 15, 32); hence, BCSCs are considered to be critical therapeutic targets (30, 33, 34). Recent studies have indicated that BCSC-enriched populations give rise to mammospheres in anchorage-independent conditions (11, 12). An understanding of the molecular mechanisms involved in the regulation of mammosphere formation is important for the design of efficient therapeutic strategies and improvements in conventional anticancer treatments. Recently, several inflammatory chemokines have been found to play a role in regulating the mammosphere-forming ability of breast cancer cells (18). However, the molecular pathways linking inflammation to mammosphere-forming ability are still largely unknown. In the present study, we describe one such molecular pathway that involves HRG, PI3K/Akt, NF-κB, and IL8.

HRG is widely expressed in numerous tissues, including breast, brain, heart, skeletal muscle, liver, and lung, and it is implicated in the regulation of a variety of biological processes, including cell proliferation, apoptosis and differentiation (35). We have identified yet another role of HRG in human breast cancer: induction of the mammosphere-forming capacity of BCSC-enriched populations. We demonstrated that the effects of HRG on mammosphere formation are mediated through a PI3K/NF-κB pathway in breast cancer cell lines and primary tumor cells derived from surgically resected breast cancer tissues. The first step of HRG stimulation is activation of PI3K, followed by the phosphorylation of Akt, which occurs within 10 min after treatment with HRG. Activated Akt phosphorylates IKKα/β and then leads to phosphorylation of IκBα, resulting in NF-κB activation. Once the signal has been activated, production of IL8 is induced at high levels. IL8 increases the self-renewal capacity of BCSC-enriched populations through nuclear translocation of β-catenin (36), indicating that the HRG/NF-κB pathway-mediated initiation of

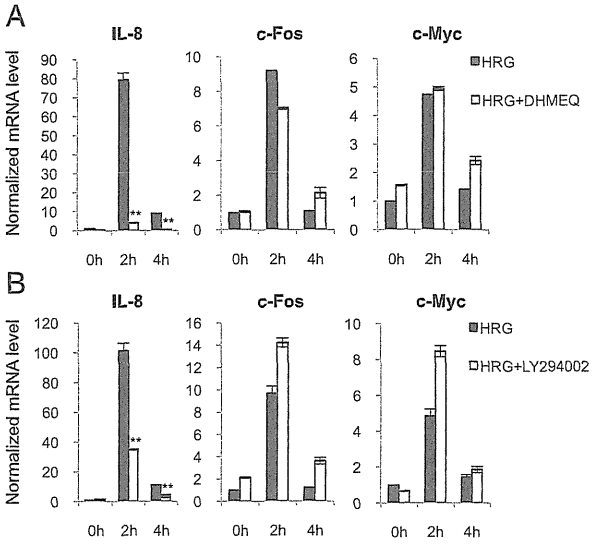

Fig. 4. IL8 is a transcriptional target of NF-κB. (*A* and *B*) MCF7 cells were treated with 5 μg/mL DHMEQ or 5 μM LY294002 for 2 hours, and then the cells were treated with 100 ng/mL HRG for 2 h and 4 h. Expression levels of *IL8*, *c-Fos*, and *c-Myc* were examined by quantitative RT-PCR (data are mean ± SD; $n = 3$, $^{**}P < 0.01$, relative to the values in the respective controls).

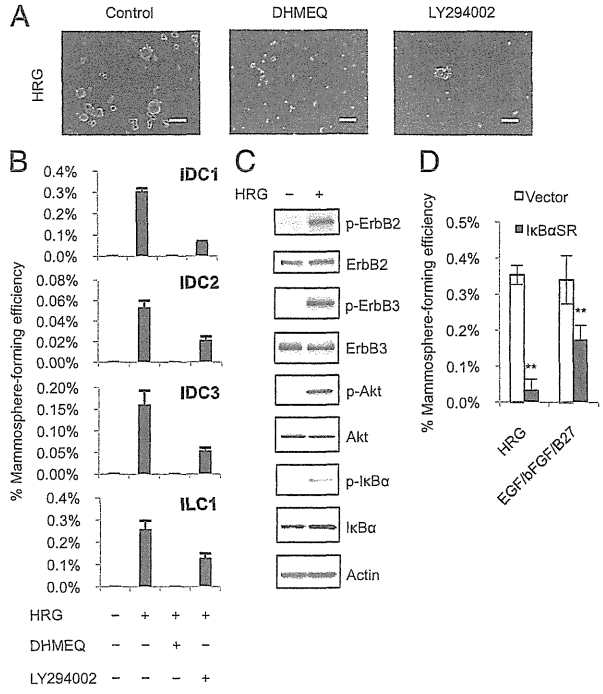

Fig. 5. The HRG/PI3K/NF-κB axis controls mammosphere formation of primary tumor cells derived from breast cancer patients. (*A*) Representative images of primary cultures of mammospheres incubated with 20 ng/mL HRG, 5 μg/mL DHMEQ and 5 μM LY294002. Scale bar = 100 μm. (*B*) Primary breast cancer cells obtained from specimens of invasive ductal carcinoma (IDC1, 2, and 3) or invasive lobular carcinoma (ILC1) were treated as indicated in *A*, and the percentage of mammosphere-forming cells was determined (data are mean ± SD; $n = 4$). (*C*) Cells from IDC1 were incubated with 100 ng/mL HRG for 10 min, and protein expression levels were determined by immunoblotting. (*D*) Cells from IDC1 expressing the indicated lentiviral vectors were incubated with 20 ng/mL HRG or with EGF/bFGF/B27, and the percentage of mammosphere-forming cells was determined (data are mean ± SD; $n = 4$, $^{**}P < 0.01$, relative to the values in the respective controls).

mammosphere formation is regulated by this pathway, at least in part. Together, these observations suggest a tight link between the HRG-induced mammosphere formation and the NF-κB–dependent inflammatory signaling pathway.

NF-κB is a central regulator of inflammatory gene expression (37). The findings presented here describe an important role of NF-κB in regulating mammosphere formation. NF-κB was activated by HRG stimulation as well as by culture with EGF/bFGF/B27, and it regulated the mammosphere formation under each culture condition. Down-regulation of NF-κB led to a decreased frequency of tumor initiation of MCF7 cells and mammosphere formation, and the cells that had low NF-κB activity showed a decreased frequency of mammosphere formation. These observations suggest that NF-κB activity is required to maintain the mammosphere-forming ability of breast cancer cells.

ErbB3 is the only ErbB family member that directly binds to PI3K (38). As ErbB3 has six direct binding sites for p85, a subunit of PI3K, the signaling output of ErbB3 is dominated by activation of the PI3K cascade, leading to activation of Akt. Although ErbB3 lacks intrinsic kinase activity, it is well known that ErbB family members homodimerize or heterodimerize to activate signaling pathways. Among the various combinations of family members, the ErbB2/ErbB3 heterodimer is considered the most potent ErbB pair with respect to the strength of interaction, ligand-induced tyrosine phosphorylation, and downstream signaling (39). Because there is no ligand for ErbB2, HRG is among the most efficient ligands to activate ErbB2/ErbB3 heterodimers. This could be the reason why HRG stimulates strong activation of the PI3K/NF-κB pathway for the mammosphere formation of breast cancer cells.

Trastuzumab (Herceptin, Genentech), a humanized monoclonal antibody directed at the ErbB2 ectodomain, is effective in the treatment of some human breast cancers that overexpress ErbB2 (40). In this study, we showed that the HRG signaling pathway plays important roles for mammosphere formation in primary tumor cells derived from human breast cancer tissues in which ErbB2 was expressed at moderate levels (Table S1) as well as in breast cancer cell lines in which ErbB2 was expressed at various levels. This raises the intriguing possibility that trastuzumab effectively targets BCSCs in the breast cancer tissues in which HRG is overexpressed even if ErbB2 is expressed at moderate levels. Indeed, it was recently reported that trastuzumab sensitizes HRG-overexpressing breast cancer cells to chemotherapy (23).

In conclusion, our results suggest that HRG/ErbB/PI3K/NF-κB signaling regulates the mammosphere formation of human breast cancer cells. Hence, in the future it will be important to develop compounds or antibodies targeted at the signaling molecules involved in this pathway to improve the prognosis of breast cancer patients.

Materials and Methods

Cell Lines and Primary Cell Culture. Breast cancer cell lines MCF7, T47D, BT20 HCC1954, and HCC1143 were purchased from the American Type Culture Collection (ATCC). Cells were cultured in RPMI1640 with 10% (vol/vol) FBS. Primary cultures of tumor cells and mammospheres were generated as described previously (12–14). Briefly, tumor samples were processed within 1 h after surgical resection. Minced pieces of human breast tumor samples were digested with 2 mg/mL collagenase A (Roche), 1 mM $CaCl_2$, and DNaseI (Roche) in RPMI1640 with 10% FBS. Tumors were digested for 1.5–2.5 h at 37 °C with shaking and pipetting every 30 min for mechanical dissociation. Once tumors were digested, the resulting single-cell suspension was filtered through a 100-μm and 40-μm cell strainer (BD Falcon) and washed with PBS. After isolation of lineage-negative (Lin^-) breast cancer cells, cells were cultured in human mammary epithelial cell growth medium (HuMEC, GIBCO) or in mammosphere culture medium, which consisted of serum-free Dulbecco's modified Eagle's Medium:Nutrient

Mixture F-12 (DMEM/F-12) medium (GIBCO) supplemented with 20 ng/mL EGF (Millipore), 20 ng/mL bFGF (PeproTech), B27 (GIBCO), and heparin (Stem Cell Technologies). B27 supplement has been shown to support the growth of mammospheres from human breast tissue (41). Alternatively, mammospheres were grown in DMEM/F12 medium supplemented with 20 ng/mL HRG-β1 (R&D).

Human breast carcinoma specimens were obtained from the University of Tokyo Hospital and Showa General Hospital. This study was approved by the institutional review boards of the Institute of Medical Science, University of Tokyo, and Showa General Hospital.

Cell Isolation. To isolate Lin^- breast cancer cells, cells obtained from breast tumor specimens were incubated with a mixture of biotin-conjugated antibodies against Lin^+ cells. The mixture of antibodies included a MACS lineage depletion kit for hematopoietic and erythrocyte precursor cells (CD2, CD3, CD11b, CD14, CD15, CD16, CD19, CD56, CD123, and CD235a, Miltenyi Biotec), CD31 (for endothelial cells, eBioscience) and CD140b (for stromal cells, Biolegend) antibody. After incubation, cells were separated using the MACS magnetic cell separation system according to the manufacturer's instructions (Miltenyi Biotec). To isolate putative stem cells, Lin^- breast cancer cells were then sorted after staining with CD24-FITC or CD44-PE antibody (BD Pharmingen) using a FACSAria Cell Sorter (BD Bioscience). Dead cells were excluded by propidium iodide (PI, Sigma) staining. Data were analyzed by FlowJo software.

Mammosphere Assay. Cells were plated as single cells in ultralow attachment plates at a low density (5,000 cells/mL) and were grown in mammosphere culture medium with or without NF-κB inhibitor DHMEQ (28), PI3K inhibitor LY294002 (Cell Signaling), lapatinib (Selleck Chemicals), gefitinib (AstraZeneca), dasatinib (Selleck Chemicals), or sunitinib (Sigma-Aldrich) at the indicated concentrations for 4–7 d. To test whether the low-density conditions, such as 5,000 cells/mL, represented clonal expansion rather than aggregation, as previously reported (11), we performed mammosphere assays using primary tumor cells from patients under the condition of 50 cells/well in 96-well plates (*SI Materials and Methods*). We found a comparable frequency of mammosphere formation irrespective of cell-plating density, strongly suggesting that mammospheres are not formed by simple cell aggregation but by clonal expansion of single cells. To culture secondary mammospheres, primary mammospheres were collected by gentle centrifugation (400 × *g*), and cells were dissociated enzymatically and mechanically into a single-cell suspension. The single-cell suspension was replated as described above.

Statistical Analysis. All data were presented as mean ± SD. The unpaired Student *t* test was used for the statistical analysis. *P* values less than 0.05 were considered statistically significant.

ACKNOWLEDGMENTS. We thank H. Nakauchi and Y. Ishii for their help with flow cytometry, N. Yamaguchi for preparing the IκBαSR construct, N. Haraguchi for advising on the design of the in vivo experiments, T. Haraguchi for advising on the generation of the lentiviruses, and Y. Murakami, H. Kawahara and M. Kuroda for preparing the H&E sections. This work was supported by a grant from the Ministry of Health, Labor and Welfare of Japan for the Third Term Comprehensive 10-Year Strategy for Cancer Control; by a Grant-in-Aid from the Ministry of Education, Science, Sports and Culture of Japan for Scientific Research on Innovative Areas; and by grants from the Cell Science Research Foundation.

1. Reya T, Morrison SJ, Clarke MF, Weissman IL (2001) Stem cells, cancer, and cancer stem cells. *Nature* 414:105–111.
2. Gotoh N (2011) Potential signaling pathways activated in cancer stem cells in breast cancer. *Cancer Stem Cells Theories and Practice*, ed Shostak S (InTech, Vienna, Austria), p 6.
3. Al-Hajj M, Wicha MS, Benito-Hernandez A, Morrison SJ, Clarke MF (2003) Prospective identification of tumorigenic breast cancer cells. *Proc Natl Acad Sci USA* 100: 3983–3988.
4. Boiko AD, et al. (2010) Human melanoma-initiating cells express neural crest nerve growth factor receptor CD271. *Nature* 466:133–137.
5. Bonnet D, Dick JE (1997) Human acute myeloid leukemia is organized as a hierarchy that originates from a primitive hematopoietic cell. *Nat Med* 3:730–737.
6. Chan KS, et al. (2009) Identification, molecular characterization, clinical prognosis, and therapeutic targeting of human bladder tumor-initiating cells. *Proc Natl Acad Sci USA* 106:14016–14021.
7. Dalerba P, et al. (2007) Phenotypic characterization of human colorectal cancer stem cells. *Proc Natl Acad Sci USA* 104:10158–10163.
8. O'Brien CA, Pollett A, Gallinger S, Dick JE (2007) A human colon cancer cell capable of initiating tumour growth in immunodeficient mice. *Nature* 445:106–110.
9. Prince ME, et al. (2007) Identification of a subpopulation of cells with cancer stem cell properties in head and neck squamous cell carcinoma. *Proc Natl Acad Sci USA* 104: 973–978.
10. Singh SK, et al. (2003) Identification of a cancer stem cell in human brain tumors. *Cancer Res* 63:5821–5828.
11. Cordenonsi M, et al. (2011) The Hippo transducer TAZ confers cancer stem cell-related traits on breast cancer cells. *Cell* 147:759–772.
12. Pece S, et al. (2010) Biological and molecular heterogeneity of breast cancers correlates with their cancer stem cell content. *Cell* 140:62–73.
13. Dontu G, et al. (2003) In vitro propagation and transcriptional profiling of human mammary stem/progenitor cells. *Genes Dev* 17:1253–1270.
14. Ponti D, et al. (2005) Isolation and in vitro propagation of tumorigenic breast cancer cells with stem/progenitor cell properties. *Cancer Res* 65:5506–5511.
15. Yu F, et al. (2007) let-7 Regulates self renewal and tumorigenicity of breast cancer cells. *Cell* 131:1109–1123.
16. Scheel C, et al. (2011) Paracrine and autocrine signals induce and maintain mesenchymal and stem cell states in the breast. *Cell* 145:926–940.
17. Hsing CH, et al. (2011) Anesthetic propofol reduces endotoxic inflammation by inhibiting reactive oxygen species-regulated Akt/IKKβ/NF-κB signaling. *PLoS ONE* 6: e17598.
18. Hinohara K, Gotoh N (2010) Inflammatory signaling pathways in self-renewing breast cancer stem cells. *Curr Opin Pharmacol* 10:650–654.
19. Murohashi M, et al. (2010) Gene set enrichment analysis provides insight into novel signalling pathways in breast cancer stem cells. *Br J Cancer* 102:206–212.
20. Hayes NV, Gullick WJ (2008) The neuregulin family of genes and their multiple splice variants in breast cancer. *J Mammary Gland Biol Neoplasia* 13:205–214.
21. Krane IM, Leder P (1996) NDF/heregulin induces persistence of terminal end buds and adenocarcinomas in the mammary glands of transgenic mice. *Oncogene* 12: 1781–1788.
22. Atlas E, et al. (2003) Heregulin is sufficient for the promotion of tumorigenicity and metastasis of breast cancer cells in vivo. *Mol Cancer Res* 1:165–175.
23. Menendez JA, Mehmi I, Lupu R (2006) Trastuzumab in combination with heregulin-activated Her-2 (erbB-2) triggers a receptor-enhanced chemosensitivity effect in the absence of Her-2 overexpression. *J Clin Oncol* 24:3735–3746.
24. Dunn M, et al. (2004) Co-expression of neuregulins 1, 2, 3 and 4 in human breast cancer. *J Pathol* 203:672–680.
25. Korkaya H, Paulson A, Iovino F, Wicha MS (2008) HER2 regulates the mammary stem/progenitor cell population driving tumorigenesis and invasion. *Oncogene* 27: 6120–6130.
26. Ginestier C, et al. (2007) ALDH1 is a marker of normal and malignant human mammary stem cells and a predictor of poor clinical outcome. *Cell Stem Cell* 1:555–567.
27. Mani SA, et al. (2008) The epithelial-mesenchymal transition generates cells with properties of stem cells. *Cell* 133:704–715.
28. Nishimura D, et al. (2006) DHMEQ, a novel NF-kappaB inhibitor, induces apoptosis and cell-cycle arrest in human hepatoma cells. *Int J Oncol* 29:713–719.
29. Charafe-Jauffret E, et al. (2009) Breast cancer cell lines contain functional cancer stem cells with metastatic capacity and a distinct molecular signature. *Cancer Res* 69: 1302–1313.
30. Ginestier C, et al. (2010) CXCR1 blockade selectively targets human breast cancer stem cells in vitro and in xenografts. *J Clin Invest* 120:485–497.
31. Pahl HL (1999) Activators and target genes of Rel/NF-kappaB transcription factors. *Oncogene* 18:6853–6866.
32. Diehn M, et al. (2009) Association of reactive oxygen species levels and radioresistance in cancer stem cells. *Nature* 458:780–783.
33. Gupta PB, et al. (2009) Identification of selective inhibitors of cancer stem cells by high-throughput screening. *Cell* 138:645–659.
34. Morrison BJ, Schmidt CW, Lakhani SR, Reynolds BA, Lopez JA (2008) Breast cancer stem cells: Implications for therapy of breast cancer. *Breast Cancer Res* 10:210.
35. Stove C, Bracke M (2004) Roles for neuregulins in human cancer. *Clin Exp Metastasis* 21:665–684.
36. Liu S, Wicha MS (2010) Targeting breast cancer stem cells. *J Clin Oncol* 28:4006–4012.
37. Karin M, Greten FR (2005) NF-kappaB: Linking inflammation and immunity to cancer development and progression. *Nat Rev Immunol* 5:749–759.
38. Hynes NE, Lane HA (2005) ERBB receptors and cancer: The complexity of targeted inhibitors. *Nat Rev Cancer* 5:341–354.
39. Olayioye MA, Neve RM, Lane HA, Hynes NE (2000) The ErbB signaling network: Receptor heterodimerization in development and cancer. *EMBO J* 19:3159–3167.
40. Vogel CL, et al. (2002) Efficacy and safety of trastuzumab as a single agent in first-line treatment of HER2-overexpressing metastatic breast cancer. *J Clin Oncol* 20:719–726.
41. Lim E, et al.; kConFab (2009) Aberrant luminal progenitors as the candidate target population for basal tumor development in BRCA1 mutation carriers. *Nat Med* 15: 907–913.

American Journal of Transplantation 2012; 12: 102–114
Wiley Periodicals Inc.

doi: 10.1111/j.1600-6143.2011.03771.x

Rapamycin Causes Upregulation of Autophagy and Impairs Islets Function Both *In Vitro* and *In Vivo*

M. Tanemura[a,*], Y. Ohmura[a], T. Deguchi[a], T. Machida[a], R. Tsukamoto[a], H. Wada[a], S. Kobayashi[a], S. Marubashi[a], H. Eguchi[a], T. Ito[b], H. Nagano[a], M. Mori[a] and Y. Doki[a]

Departments of [a] Gastroenterological Surgery and [b] Complementary and Alternative Medicine, Osaka University Graduate School of Medicine, Osaka, Japan
**Corresponding author: Masahiro Tanemura, mtanemura@gesurg.med.osaka-u.ac.jp*

Autophagy is a lysosomal degradation process of redundant or faulty cell components in normal cells. However, certain diseases are associated with dysfunctional autophagy. Rapamycin, a major immunosuppressant used in islet transplantation, is an inhibitor of mammalian target of rapamycin and is known to cause induction of autophagy. The objective of this study was to evaluate the *in vitro* and *in vivo* effects of rapamycin on pancreatic β cells. Rapamycin induced upregulation of autophagy in both cultured isolated islets and pancreatic β cells of green fluorescent protein–microtubule-associated protein 1 light chain 3 transgenic mice. Rapamycin reduced the viability of isolated β cells and down-regulated their insulin function, both *in vitro* and *in vivo*. In addition, rapamycin increased the percentages of apoptotic β cells and dead cells in both isolated and *in vivo* intact islets. Treatment with 3-methyladenine, an inhibitor of autophagy, abrogated the effects of rapamycin and restored β-cell function in both *in vitro* experiments and animal experiments. We conclude that rapamycin-induced islet dysfunction is mediated through upregulation of autophagy, with associated downregulation of insulin production and apoptosis of β cells. The results also showed that the use of an autophagy inhibitor abrogated these effects and promoted islet function and survival. The study findings suggest that targeting the autophagy pathway could be beneficial in promoting islet graft survival after transplantation.

Key words: Autophagy, islet transplantation, LC3, rapamycin, transgenic mice

Abbreviations: Atg gene, autophagy related gene; BSA, bovine serum albumin; FKBP-12, 12-kDa FK506-binding protein; GFP, green fluorescent protein; GAPDH, glyceraldehyde-3-phosphate; LC3, microtubule-associated protein 1 light chain 3; mTOR, mammalian target of rapamycin; PBS, phosphate-buffered saline; TUNEL, terminal deoxynucleotidyl transferase-mediated dUTP nick-end labeling; SD, standard deviation.

Received 18 March 2011, revised 22 August 2011 and accepted for publication 22 August 2011

Introduction

Autophagy, i.e. "self-eating", is an intracellular degradation system designed for degradation of cytoplasmic proteins and dysfunctional organelles after their sequestration in the autophagosome. To date, only microtubule-associated protein1 light chain 3 (LC3), a mammalian homolog of yeast autophagy related gene8 (Atg8), is known to exist in the autophagosomes, and therefore this protein serves as a marker for autophagosomes (1–3). The process is tightly regulated and plays an important role in cell growth, development and homeostasis, where it helps to maintain a balance between the synthesis, degradation and subsequent recycling of cellular components (1–3). Autophagy is induced dynamically by nutrient depletion to provide necessary amino acids within cells, thus helping them adapt to starvation (4). The physiological role of autophagy has been studied in various organisms and current knowledge indicates that autophagy is involved not only in adaptation to starvation but also in the quality control of intracellular proteins and organelles, to maintain cell functions, development, growth, clearance of intracellular microbes, antigen presentation and protection against disease (5–11). Thus, autophagy functions as a cell-protective mechanism and is up-regulated when cells are preparing to rid themselves of damaging cytoplasmic components, for example, during infection or protein aggregate accumulation (12).

Rapamycin is a macrolide fungicide with immunosuppressant properties that bear molecular structural similarities to the calcineurin inhibitor, tacrolimus (13). However, the mechanism of action of rapamycin is distinct from that of calcineurin inhibitor, such as cyclosporine and tacrolimus. Rapamycin binds to its intracellular receptor, the immunophilin 12-kDa FK506-binding protein (FKBP-12) and the rapamycin-FKBP-12 complex binds to and inhibits the mammalian target of rapamycin (mTOR; Ref. 14). Inhibition of mTOR leads to arrest of the cell cycle at the G1 to S phase and thus, blockade of growth-factor-driven proliferation of not only activated T cells, which constitute the basis of its immunosuppressive action, but also

other hematopoietic and nonhematopoietic cells (14,15). The mTOR is ubiquitously expressed in various cell types and functionally is a serine/threonine protein kinase that regulates important cellular process, including growth, proliferation, motility, survival, protein synthesis and transcription (16). Furthermore, activation of mTOR leads to inhibition of autophagy in cells ranging from yeast to human (17). Based on the above background, it is conceivable that the inhibitory action of rapamycin on mTOR activity induces autophagy in pancreatic islets.

Islet transplantation was recently advanced by the publication of the results of the Edmonton Protocol of immunosuppressive regimen, leading to insulin independence at 1 year in 90% of patients treated with type 1 diabetes (18–21). Accordingly, rapamycin has become a part of the standard treatment in islet transplantation. Its effectiveness in preventing allorejection and autoimmunity and promoting the survival of regulatory T lymphocytes has contributed to widespread use (22–24). However, recent reports described gradual deterioration of the metabolic profile and the need for reintroduction of exogenous insulin; only 10% of islet recipients maintained insulin independence at 5 years (21,25,26). Although the cause of the decline in insulin independence rates after islet transplantation remains obscure, the decline may reflect toxicity associated with long-term use of immunosuppressive drugs on islet β cells.

The effects of calcineurin inhibitors on islet function and proliferation have been recognized (27,28), although increasing data suggest that rapamycin alone or in combination with tacrolimus could impair islet cell function and survival (29–31). In addition, the antiangiogenic and antiproliferative properties of rapamycin could also prevent vascularization of transplanted islets, with a resultant reduction of posttransplantation engrafted and surviving islet mass (32–34).

Although it has been reported that β cells of ZDF rats (a rodent model of type 2 diabetes) contain a significant number of autophagic vacuoles (35), there is little information on the physiopathological roles of autophagy in the islets, and no causal link has been reported between autophagy and pathogenesis of diabetes. The aims of this study were to evaluate the *in vitro* and *in vivo* effects of rapamycin on pancreatic β cells, including induction of autophagy, cell viability and insulin secretory function, because these factors may contribute to progressive dysfunction of islet grafts in recipients.

Materials and Methods

In vitro *autophagy induction assay and islet viability assay*

Thirty cells from fresh mice islets, obtained from either C57BL/6 mice or green fluorescent protein (GFP)–LC3 transgenic mice were seeded in a 96-well culture plate and cultured for either 24 or 48 h with complete culture medium containing 1 or 10 ng/mL of rapamycin. In the first step, treated islets that were isolated from transgenic mice were observed by fluorescence microscopy to detect GFP signals, which is an accurate marker of induction of autophagy (36). Subsequently, islet viability was evaluated after 24 h treatment by monitoring metabolic activity with the colorimetric methyl tetrazolium salt (MTS) assay using the Cell Titer 96 Aqueous One reagent (Promega, Madison, WI, USA; Ref. 37). The colorimetric reagent was added to each well of the plate and incubated for 2 h, and the absorbance values read at 490 nm.

To further determine the change in islet viability before/after rapamycin treatment, fluorescence labeling was performed using tetramethyl rhodamine ethyl ester (TMRE; Molecular Probes, Eugene, OR, USA) and 7-amino actinomycin D (7-AAD; Molecular Probes; Refs. 38,39). Islets treated or untreated with rapamycin were dissociated into single cell suspensions, using Accutase (Innovative Cell Technologies Inc, San Diego, CA, USA). The dispersed cell suspensions were stained with Newport Green PDX acetoxymethylether (Molecular Probes), for identification of β cells (38). The single islet cell suspensions were incubated with 100 ng/mL TMRE for 30 min at 37°C in phosphate-buffered saline (PBS) without Ca^{2+} and Mg^{2+}. This dye selectively binds to the mitochondrial membrane allowing the assessment of cells with functional mitochondria, and therefore is a good marker for cell viability. Furthermore, cells were stained with 7-AAD that binds to DNA when cell membrane permeability is altered after cell death. Stained cells were analyzed by FACSCalibur flow cytometer (BD Immunocytometry, San Jose, CA, USA). In addition, improvement in islet viability was assessed by either MTS assay, TMRE or 7-AAD staining based on the results of autophagic signal blocking. Islet viability assays were performed with the addition of 10 mM of 3-methyladenine (3-MA).

Glucose-stimulated insulin release and stimulation index (SI)

To determine the changes in the endocrinological potency of rapamycin-treated islets, static glucose challenge was performed with or without 1 or 10 ng/mL of rapamycin. After overnight culture with or without rapamycin, 100 IEQ of treated islets were incubated with either 2.8 or 20 mM of glucose in culture medium for 2 h at 37°C to stimulate insulin release. The supernatants were collected and stored at −80°C for insulin assessment by enzyme-linked immunosorbent assay (ELISA; Mercodia Inc., Uppsala, Sweden; Refs. 38–40). Glucose-stimulated insulin release was expressed as the SI, calculated as the ratio of insulin released during exposure to high glucose (20 mM) over that released during low glucose incubation (2.8 mM). To determine the *in vitro* islet potency with regard to autophagic signal blocking, static incubation was also performed with the addition of 10 mM of 3-MA.

In vivo *studies using GFP-LC3 transgenic mice*

To study the effects of starvation, transgenic mice were provided with drinking water *ad libitum*, but were deprived of food for 24 h (10 a.m.–10 a.m.; Ref. 36). The starved transgenic mice were sacrificed and the pancreas, brain and muscle tissues were recovered. This was followed by preparation of the tissues for fluorescence microscopy. Furthermore, to demonstrate *in vivo* 3-MA-induced blocking of autophagy, mice were injected intraperitoneally (i.p.) with 10 mM of 3-MA for 2 weeks, followed by starvation for 24 h.

To assess the *in vivo* effects of rapamycin on islets from GFP-LC3 transgenic mice, mice were randomly separated into three experimental groups, no treatment group (i.e. control group; n = 25), rapamycin-treated group (n = 25) and the combination treatment group (n = 25) treated with both rapamycin and 3-MA. Rapamycin treatment consisted of daily i.p. injection of 0.2 mg/kg rapamycin and combined treatment consisted of daily i.p. injection of 0.2 mg/kg rapamycin combined with 10 mM of 3-MA. These treatments continued for 1, 2, 3, 4 or 5 weeks (n = 5 mice, each). The rapamycin-treated transgenic mice were sacrificed, the pancreas was removed and